ISSN: 2632-9417

INTERNATIONAL JOURNAL OF PHYSICS & MATHEMATICS

VOLUME NO. 7
ISSUE NO. 1
JANUARY - APRIL 2024

ENRICHED PUBLICATIONS

EIS LEARNING
No - 198, Upper Hatia, Near Mahatma Gandhi
Smarak High School, Ranchi - 834003, Jharkhand
Ph : 919097302256 / Email : info@eislearning.com

ISSN: 2632-9417

International Journal of Physics & Mathematics

Aim & Scope

Aims

IJPM publishes papers in theoretical physics which present a rigorous mathematical approach to problems of quantum and classical mechanics and field theories, relativity and gravitation, statistical physics and mathematical foundations of physical theories. Papers using modern methods of functional analysis, probability theory, differential geometry, algebra, and mathematical logic are preferred.

Scope

Acoustics & Sound

Algebra

Astronomy & Astrophysics

Biophysics

Computational Mathematics

Condensed Matter Physics & Semiconductors

Discrete Mathematics

Electromagnetism

Fluid Mechanics

Geometry

Geophysics

High Energy & Nuclear Physics

Mathematical Analysis

Mathematical Optimization

Mathematical Physics

Nonlinear Science

Optics & Photonics

Plasma & Fusion

Probability & Statistics with Applications

Pure & Applied Mathematics

Quantum Mechanics

Spectroscopy & Molecular Physics

Thermal Sciences

ISSN: 2632-9417

Editor-in-Chief

Chief Executive Editor

Associate Editor

International Advisory Board

ISSN: 2632-9417

International Journal of Physics & Mathematics

(Volume No. 7, Issue No. 1, January - April 2024)

Contents

Sr. No.	Article / Authors Name	Pg. No.
1	Influence of Hall Current and Rotation on the Radiative MHD Flow Past an Impulsively Started Infinite Vertical Porous Plate *- P Bhaskar, M Venkateswarlu*	1 - 14
2	Parameter Estimation of Inverted Exponential Distribution Via Bayesian Approach *- Arun Kumar Rao, Himanshu Pandey*	15 - 22
3	A Study of Formation and Evolution of Black Hole *- Neeraj Kumar Mishra, Priyanka Vaidya*	23 - 30
4	An Evaluation of Thermal Conductivity of High-Temperature Superconductors *- Neeraj Kumar Mishra, Priyanka Vaidya*	31 - 36

ISSN: 2632-9417

Influence of Hall Current and Rotation on the Radiative MHD Flow Past an Impulsively Started Infinite Vertical Porous Plate

P Bhaskar[1], M Venkateswarlu[2]

[1]Research Scholar, Department of Mathematics, S. V. University, Gajraula, Uttar Pradesh, India
[2]Department of Mathematics, V. R. Siddhartha Engineering College, Vijayawada, Andhra Pradesh, India

ABSTRACT

The present investigation deals with the effects of hall current, and Soret number on the non linear, radiative, unsteady, hydromagnetic natural convection flow of an optically thick rotating fluid past an impulsively started vertical porous plate. Exact analytical solution of the non-dimensional governing equations is obtained in closed form by using Laplace transform technique. The numerical values of primary and secondary velocity profiles are displayed graphically for different values of pertinent flow parameters.

Keywords: hall current, rotation, radiation, hydromagnetic, soret effect

1. INTRODUCTION

The Hall current aspect has an important role in many engineering applications. Several scientific and engineering processes involve the flow and mechanism of fluid-particle mixtures. Particular examples of such processes are the blood flow in arteries, combustion, wastewater treatment, cement production, flows in rocket tubes, steel manufacturing industry, dust in gas cooling systems, movement of inert solid particles in the atmosphere etc. Seth et al. [1] studied the effects of hall current and rotation on unsteady MHD natural convection flow with heat and mass transfer past an impulsively moving vertical plate in the presence of radiation and chemical reaction. Venkateswarlu et al. [2] studied the Dufour and heat source effects on radiative MHD slip flow of a viscous fluid in a parallel porous plate channel in presence of chemical reaction. Reddy et al. [3] presented the influence of thermal radiation, viscous dissipation and hall current on MHD convection flow over a stretched vertical flat plate. Venkateswarlu et al. [4] studied the influence of thermal radiation and heat generation on steady hydromagnetic flow in a vertical micro – porous – channel in presence of suction/injection. Vieru et al. [5] reported the magnetohydrodynamic natural convection flow with Newtonian heating and mass diffusion over an infinite plate that applies shear stress to a viscous fluid. Venkateswarlu et al. [6] discussed the influence of Hall current and heat source on MHD flow of a rotating fluid in a parallel porous plate channel. Uddin et al. [7] presented the influence of thermal radiation and heat generation or absorption on MHD heat transfer flow of a micropolar fluid past a wedge considering hall and ion slip currents. Venkateswarlu and Phani Kumar [8] studied the Soret and heat source effects on MHD flow of a viscous fluid in a parallel porous plate channel in presence of slip condition. Takhar et al. [9] presented the unsteady free convection flow over an infinite vertical porous plate due to the combined effects of thermal and mass diffusion, magnetic field and Hall currents. Malapati and Dasari [10] investigated Soret and chemical reaction effects on the radiative MHD flow from an infinite vertical plate. Seth et al [11] discussed the effects of Hall current and rotation on MHD natural convection flow past an impulsively moving vertical plate with ramped temperature in the presence of thermal diffusion with heat absorption. Venkateswarlu and Makinde [12] presented the unsteady MHD slip flow with radiative heat and mass transfer over an inclined plate embedded in a porous medium. Sattar [13] reported the unsteady hydromagnetic free convection flow with

Hall current mass transfer and variable suction through a porous medium near an infinite vertical porous plate with constant heat flux. Venkateswarlu et al. [14] considered the thermodynamic analysis of Hall current and Soret number on hydromagnetic couette flow in a rotating system with a convective boundary condition. Seth et al. [15] considered the unsteady hydromagnetic natural convection flow of a heat absorbing fluid within a rotating vertical channel in porous medium with Hall effects. Venkateswarlu et al. [16] presented the influence of heat generation and viscous dissipation on hydromagnetic fully developed natural convection flow in a vertical micro–channel. In another study, Venkateswarlu et al. [17] discussed the Soret and Dufour effects on radiative hydromagnetic flow of a chemically reacting fluid over an exponentially accelerated inclined porous plate in presence of heat absorption and viscous dissipation. The following strategy is pursued in the rest of the paper. Section two presents the formation of the problem. The analytical solutions are presented in section three and finally results are discussed in section four.

2. FORMATION OF THE PROBLEM

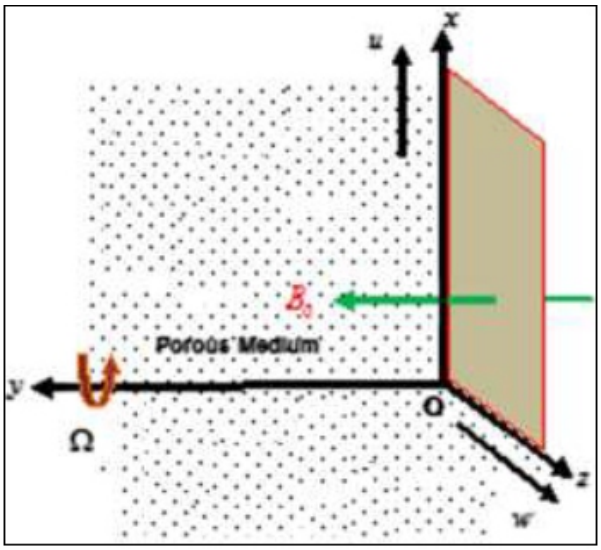

Fig 1: Geometry of the problem.

Consider the unsteady, non linear, radiative, hydromagnetic natural convection flow of an incompressible, viscous and electricity conducting fluid past a suddenly started infinite vertical porous plate in presence of a uniform transverse magnetic field of strength B_o. In view of the assumptions made by Ahmed [18], as well as of the usual Boussinesq's approximation, the dimensional governing equations can be written as

$$\frac{\partial v}{\partial y} = 0 \tag{1}$$

Momentum conservation equations:

$$\frac{\partial u}{\partial t} + 2\Omega w = \nu \frac{\partial^2 u}{\partial y^2} - \frac{\sigma B_0^2}{\rho}\left[\frac{u + mw}{1+m^2}\right] + g\beta_T\left(T - T_\infty\right) + g\beta_C\left(C - C_\infty\right) - \nu\frac{u}{K_1} \tag{2}$$

$$\frac{\partial w}{\partial t} - 2\Omega u = \nu \frac{\partial^2 w}{\partial y^2} + \frac{\sigma B_0^2}{\rho}\left[\frac{mu - w}{1+m^2}\right] - \nu\frac{w}{K_1} \tag{3}$$

Energy conservation equation:

$$\frac{\partial T}{\partial t}=\frac{k_T}{\rho c_p}\frac{\partial^2 T}{\partial y^2}-\frac{1}{\rho c_p}\frac{\partial q_r}{\partial y} \tag{4}$$

Mass diffusion equation:

$$\frac{\partial C}{\partial t}=D_M\frac{\partial^2 C}{\partial y^2}+\frac{D_M k_T}{T_M}\frac{\partial^2 T}{\partial y^2} \tag{5}$$

We should in prior warn the reader that our model is not the same as that by Ahmed [18], in which the Hall current, rotation and permeability parameters were not taken into account. Interpretation radiation term is totally different in both papers. The initial and boundary conditions for the fluid flow problem are given below

$$\left.\begin{aligned} &t\le 0: u=0, w=0,\ T=T_\infty,\ C=C_\infty\ \forall\ \ y\ge 0\\ &t>0: u=u_o, w=0, T=T_w, C=C_w\ \text{ at }\ y=0\\ &u\to 0, w\to 0, T\to T_\infty, C\to C_\infty\ \text{ as }\ y\to\infty \end{aligned}\right\} \tag{6}$$

In the case of an optically thick gray fluid, the local radiative heat flux term is simplified by using the Roseland approximation (Ahmed[18])

$$q_r=-\frac{4\sigma^*}{3a^*}\frac{\partial T^4}{\partial y} \tag{7}$$

It is assumed that the temperature difference within the fluid flow is sufficiently small such that the fluid temperature T_4 may be expressed as a linear function of the temperature. This is accomplished by expanding T_4 in a Taylor's series about free stream temperature T_∞. By neglecting second and higher order terms, T_4 is expressed as,

$$T^4\approx 4T_\infty^3 T-3T_\infty^4 \tag{8}$$

Using the equations (7) and (8) in equation (4) we obtain

$$\frac{\partial T}{\partial t}=\frac{k_T}{\rho c_p}\left[1+\frac{16\sigma^* T_\infty^3}{3a^* k_T}\right]\frac{\partial^2 T}{\partial y^2} \tag{9}$$

In order to write the governing equations and the boundary conditions in non dimensional form, the following non dimensional quantities are introduced.

$$\tau=\frac{u_o^2}{\nu}t, Y=\frac{u_o}{\nu}y, U=\frac{u}{u_o}, W=\frac{w}{u_o}, \theta=\frac{T-T_\infty}{T_w-T_\infty}, \phi=\frac{C-C_\infty}{C_w-C_\infty}, u_o=\left[g\beta_T\left(T_w-T_\infty\right)\nu\right]^{1/3} \tag{10}$$

Equations (2), (3), (5) and (9) reduce to the following non dimensional form.

$$\frac{\partial U}{\partial \tau}+2K^2W=\frac{\partial^2 U}{\partial Y^2}-\frac{M\left(mW+U\right)}{1+m^2}+\theta+N\phi-\frac{U}{K} \tag{11}$$

$$\frac{\partial W}{\partial \tau}-2K^2U=\frac{\partial^2 W}{\partial Y^2}+\frac{M(mU-W)}{1+m^2}-\frac{W}{K} \tag{12}$$

$$\frac{\partial \theta}{\partial \tau} = \left[\frac{1+R}{Pr}\right]\frac{\partial^2 T}{\partial Y^2} \tag{13}$$

$$\frac{\partial \phi}{\partial \tau} = \frac{1}{Sc}\frac{\partial^2 \phi}{\partial Y^2} + Sr\frac{\partial^2 \theta}{\partial Y^2} \tag{14}$$

We should in prior warn the reader that our model is not the same as that by Ahmed [18], in which the Hall current, rotation and permeability parameters were not taken into account. Interpretation radiation term is totally different in both papers. The initial and boundary conditions for the fluid flow problem are given below

Here $K^2 = \frac{\Omega \nu}{u_o^2}$ is the rotation parameter, $M = \frac{\sigma B_0^2 \nu}{\rho u_0^2}$ is the magnetic parameter, $K = \frac{K_1 u_0^2}{\nu^2}$ is the permeability parameter, $N = \frac{\beta_C (C_w - C_\infty)}{\beta_T (T_w - T_\infty)}$ is the ratio of the buoyancy forces due to the temperature and concentration, $Pr = \frac{\nu \rho c_p}{k_T}$ is the Prandtl number, $R = \frac{16\sigma^* T_\infty^3}{3a^* K_T}$ is the radiation parameter, $Sr = \frac{D_M k_T (T_w - T_\infty)}{T_M \nu (C_w - C_\infty)}$ is the Soret number and $Sc = \frac{\nu}{D_M}$ is the Schmidt number respectively.

The initial and boundary conditions, in equation (6) reduced to the following non-dimensional form

$$\left.\begin{aligned} &\tau \le 0 : U = 0, W = 0,\ \theta = 0, \phi = 0 \ \forall\ Y \ge 0 \\ &\tau > 0 : U = 1, W = 0, \theta = 1, \phi = 1 \text{ at } Y = 0 \\ &U \to 0, W \to 0, \theta \to 0, \phi \to 0 \text{ as } Y \to \infty \end{aligned}\right\} \tag{15}$$

By combining the equations (11) and (12), we obtain

$$\frac{\partial F}{\partial \tau} - 2iK^2 F = \frac{\partial^2 F}{\partial Y^2} - \left[\frac{M}{1+im} + \frac{1}{K}\right]F + \theta + N\phi \tag{16}$$

Here $F(\eta, \tau) = U(\eta, \tau) + iW(\eta, \tau)$

Initial and boundary conditions, in equation (15), in compact form, are given by

$$\left.\begin{aligned} &\tau \le 0 : F = 0,\ \theta = 0, \phi = 0 \ \forall\ Y \ge 0 \\ &\tau > 0 : F = 1, \theta = 1, \phi = 1 \text{ at } Y = 0 \\ &F \to 0, \theta \to 0, \phi \to 0 \text{ as } Y \to \infty \end{aligned}\right\} \tag{17}$$

3. SOLUTION OF THE PROBLEM

Now we solve the equations (13), (14) and (16) subject to the initial and boundary conditions in equation (17) by using Laplace transform technique.

Define $\eta = \frac{Y}{2\sqrt{\tau}}$ (18)

Then the equations (13), (14) and (16) are transformed into the following form

$$\frac{\partial F}{\partial \tau} - \frac{\eta}{2\tau}\frac{\partial F}{\partial \eta} - \frac{1}{4\tau}\frac{\partial^2 F}{\partial \eta^2} + \left[\frac{M}{1+im} + \frac{1}{K} - 2iK^2\right]F = \theta + N\phi \tag{19}$$

$$\frac{\partial \theta}{\partial \tau} - \frac{\eta}{2\tau}\frac{\partial \theta}{\partial \eta} - \left[\frac{1+R}{4\,Pr\,\tau}\right]\frac{\partial^2 \theta}{\partial \eta^2} = 0 \tag{20}$$

$$\frac{\partial \phi}{\partial \tau} - \frac{\eta}{2\tau}\frac{\partial \phi}{\partial \eta} - \frac{1}{4\tau Sc}\frac{\partial^2 \phi}{\partial \eta^2} = \frac{Sr}{4\tau}\frac{\partial^2 \theta}{\partial \eta^2} \tag{21}$$

The boundary conditions in equation (17) can be written as

$$\left.\begin{array}{l} F(0,\tau)=1,\quad \theta(0,\tau)=1,\quad \phi(0,\tau)=1 \\ F(\infty,\tau)=0,\ \theta(\infty,\tau)=0,\ \phi(\infty,\tau)=0 \end{array}\right\} \tag{22}$$

The exact solutions for the fluid velocity $F(\eta,\tau)$, fluid temperature $\theta(\eta,\tau)$ and species concentration $\phi(\eta,\tau)$ are obtained and are presented in the following form after simplification

$$\begin{aligned} F(\eta,\tau) = {} & a_{22}\psi_o(0,\, a_1,\, \eta,\, \tau)+Na_{17}\exp(-a_3\tau)\psi_o(-a_3,\, a_1,\, \eta,\, \tau)+ \\ & Na_{16}\exp(-a_3\tau)\left[\psi_o(-a_3,\, Sc,\, \eta,\, \tau)-\psi_o(a_7-a_3,\, 1,\, \eta,\, \tau)\right]+ \\ & a_{20}\exp(-a_{10}\tau)\left[\psi_o(a_7-a_{10},\, 1,\, \eta,\, \tau)-\psi_o(-a_{10},\, a_1,\, \eta,\, \tau)\right]+ \\ & Na_{11}\psi_o(0,\, Sc,\, \eta,\, \tau)+a_{18}\psi_o(a_7,\, 1,\, \eta,\, \tau) \\ & a_{21}\exp(a_{12}\tau)\left[\psi_o(a_7+a_{12},\, 1,\, \eta,\, \tau)-\psi_o(a_{12},\, Sc,\, \eta,\, \tau)\right]+ \end{aligned} \tag{23}$$

$$\theta(\eta,\tau)=\psi_o(0,\, a_1,\, \eta,\, \tau) \tag{24}$$

$$\begin{aligned} \phi(\eta,\tau) = {} & a_6\exp(-a_3\tau)\left[\psi_o(-a_3,\, Sc,\, \eta,\, \tau)-\psi_o(-a_3,\, a_1,\, \eta,\, \tau)\right]+ \\ & a_5\psi_o(0,\, Sc,\, \eta,\, \tau)-a_4\psi_o(0,\, a_1,\, \eta,\, \tau) \end{aligned} \tag{25}$$

Here the constants are not given under brevity.

4. RESULTS AND DISCUSSION

The numerical results are presented in Figs. 2 to 19. In the present study, the following parameter values are utilized for numerical computations: $K^2=2$, $M=1$, $m=0.5$, $K=0.2$, $N=1$, $\tau=1$, $Pr=0.71$, $R=1$, $Sr=1$ and $Sc=0.22$. Figs. 2 to 19 depict the graphs of fluid primary velocity U, secondary velocity W, temperature θ and concentration ϕ under the influence of Soret number Sr, Buoyancy parameter N, Prandtl number Pr, Schmidt number Sc, magnetic parameter M, radiation parameter R, rotation parameter K^2, Hall current parameter m and time τ.

Figs. 2 to 5 depict the influence of rotation parameter and hall current parameter on the primary velocity and secondary velocity.

It is observed that, the primary velocity decreases and secondary velocity increases on increasing the rotation parameter and hall current parameter. This implies that, rotation and hall current tends to accelerate the secondary velocity which is consistent with the fact that rotation and hall current induces secondary flow in the flow field.

Figs. 6 and 7 depict the influence of buoyancy parameter on the primary velocity and secondary velocity of the flow field. The buoyancy parameter defines the ratio of Solutal Grashof number to thermal Grashof number. It is noticed that, the primary and secondary velocities are increases on increasing the buoyancy parameter.

It is noticed that from Figs. 8 and 9, the fluid primary velocity and secondary velocity increases on increasing the radiation parameter. Figs. 10 and 11, depict the influence of Soret number on the fluid primary velocity and secondary velocity. The Soret number defines the influence of the temperature gradient inducing significant mass diffusion effects. The primary velocity and secondary velocity are found to increases on increasing the Soret number.

Figs. 12 and 13 depict the influence of magnetic parameter on the primary velocity and secondary velocity of the flow field. The transversely imposed magnetic field on the conducting dusty fluid produced a Lorentz force which acts as a resistance to the flow, consequently, the velocities decreases with an increase in magnetic parameter.

Figs. 14 and 15, shows the plot of primary velocity and secondary velocity of the flow field against different values of Prandtl number taking other parameters are constant. The Prandtl number defines the ratio of momentum diffusivity to thermal diffusivity. It is observed that, the primary velocity and secondary velocity decreases with an increase in the Prandtl number.

The influence of fluid primary velocity and secondary velocity in presence of foreign species is shown in Figs. 16 and 17.

Schmidt number signifies the relative strength of viscosity to chemical molecular diffusivity. It is observed that the primary velocity and secondary velocity decreases on increasing the Schmidt number. The flow field decelerate the velocity in presence of heavier diffusing species. It is noticed that from Figs. 18 and 19, the fluid primary velocity decreases and secondary velocity increases with the progress of time.

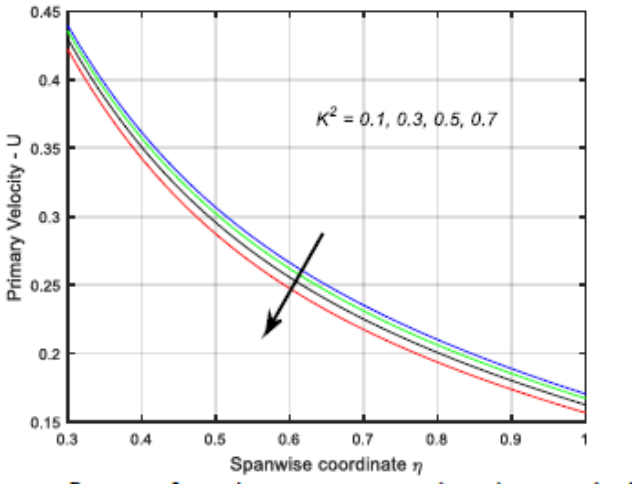

Fig 2: Influence of rotation parameter on the primary velocity.

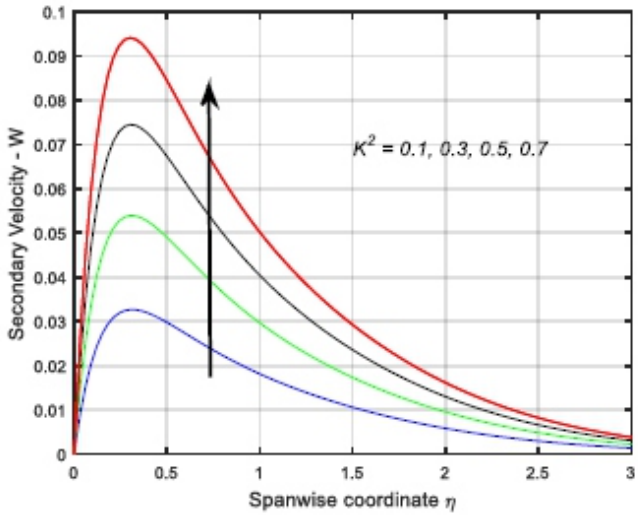

Fig. 3: Influence of rotation parameter on the secondary velocity.

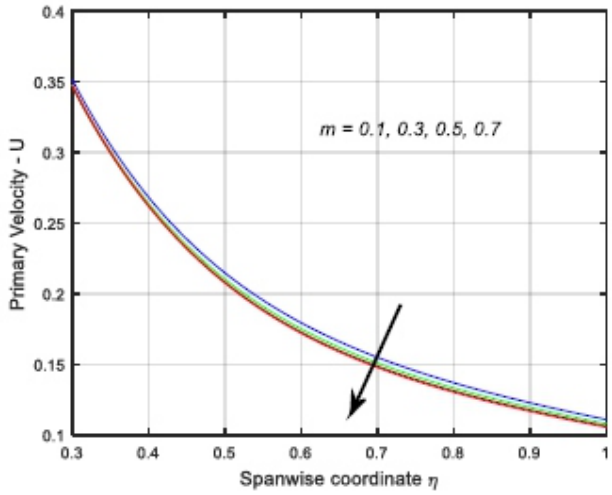

Fig 4: Influence of Hall current parameter on the primary velocity.

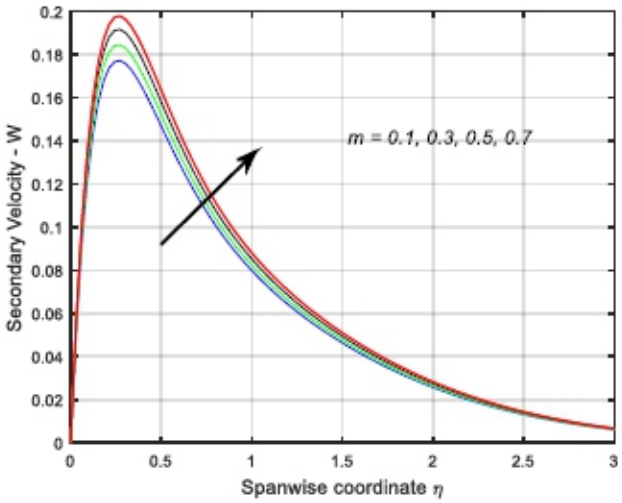

Fig 5: Influence of Hall current parameter on the secondary velocity.

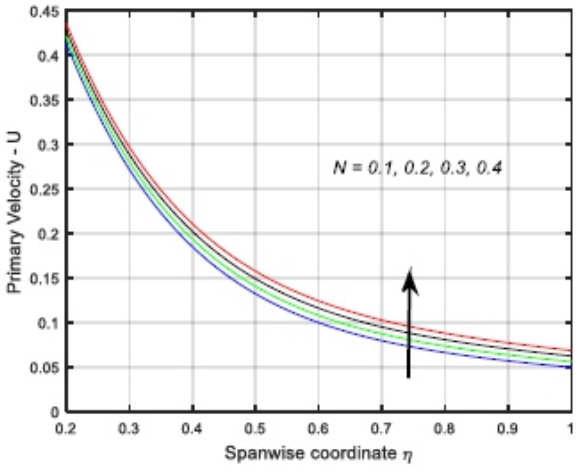

Fig 6: Influence of Buoyancy parameter on the primary velocity.

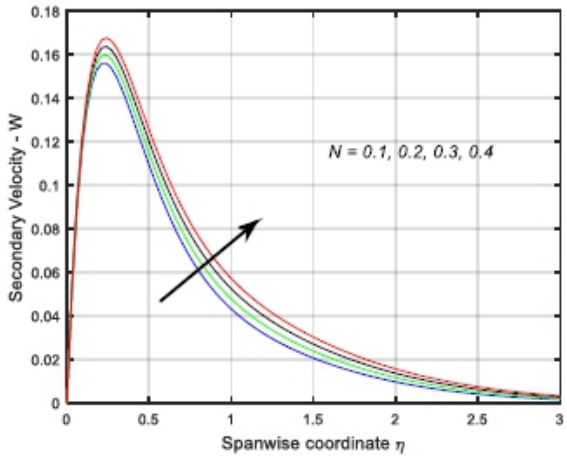

Fig 7: Influence of Buoyancy parameter on the secondary velocity.

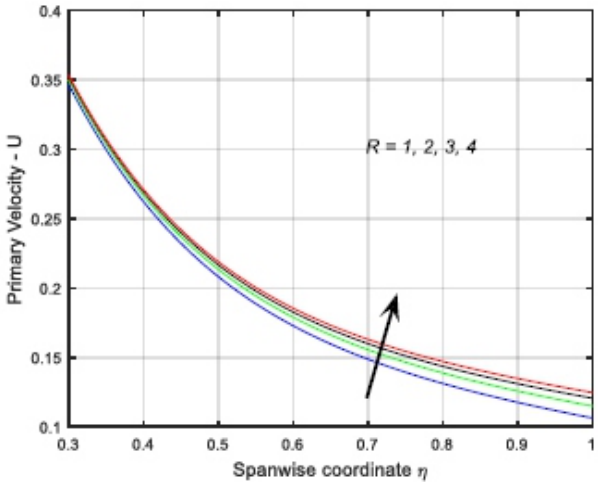

Fig 8: Influence of radiation parameter on the primary velocity.

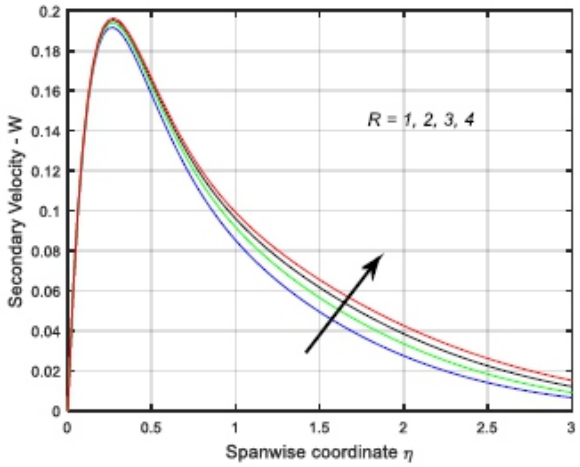

Fig 9: Influence of radiation parameter on the secondary velocity.

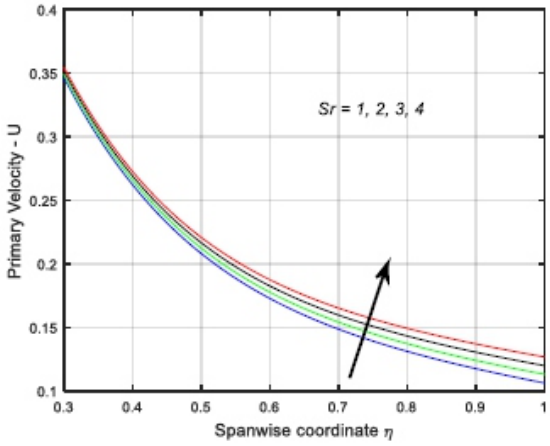

Fig 10: Influence of Soret number on the primary velocity.

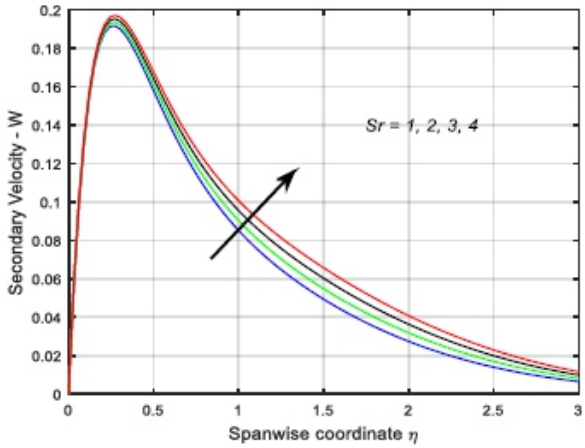

Fig 11: Influence of Soret number on the secondary velocity.

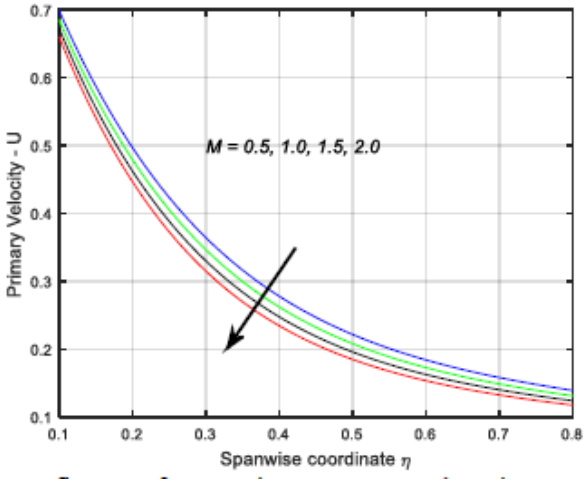

Fig 12: Influence of Magnetic parameter on the primary velocity.

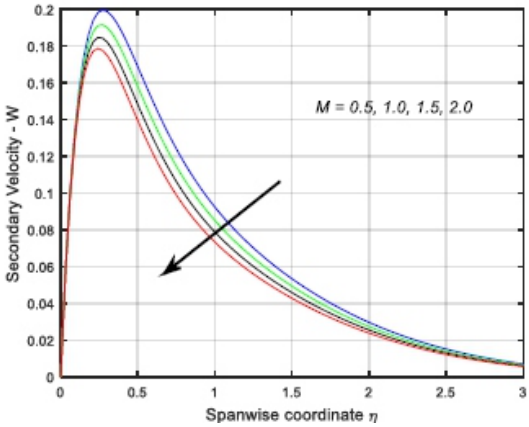

Fig 13: Influence of Magnetic parameter on the secondary velocity.

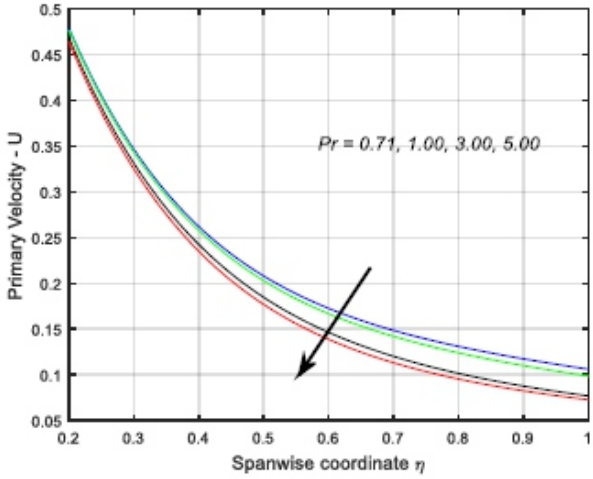

Fig 14: Influence of Prandtl number on the primary velocity.

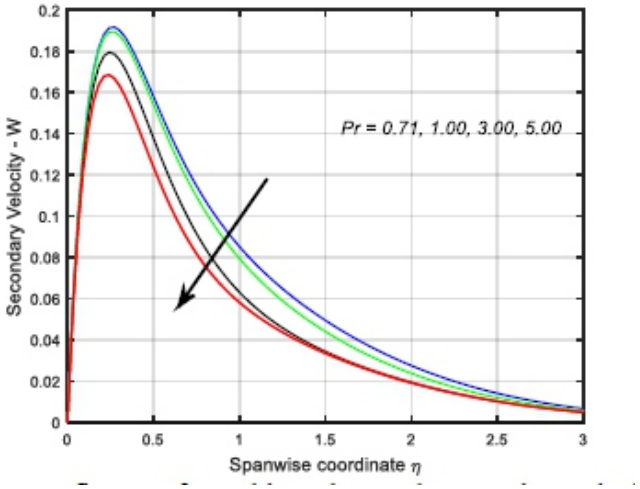

Fig 15: Influence of Prandtl number on the secondary velocity.

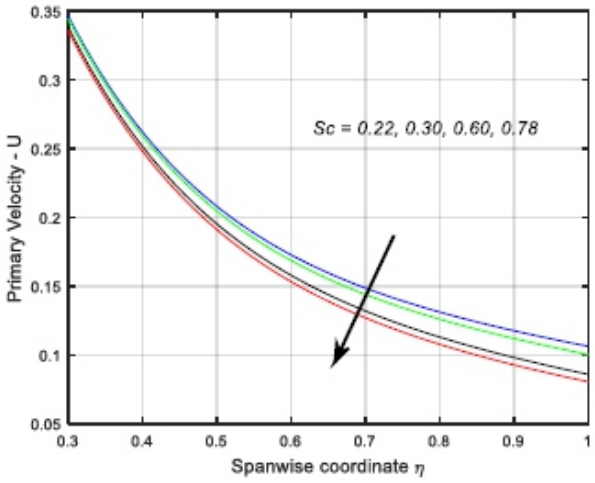

Fig 16: Influence of Schmidt number on the primary velocity.

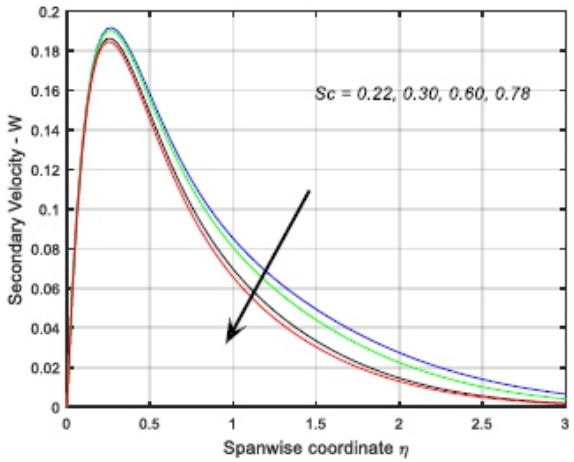

Fig 17: Influence of Schmidt number on the secondary velocity.

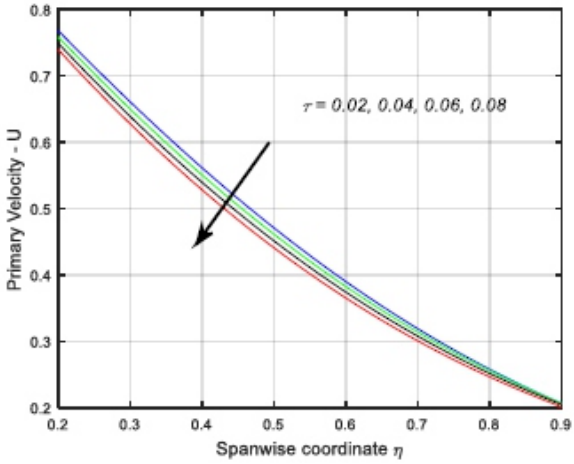

Fig 18: Influence of time on the primary velocity.

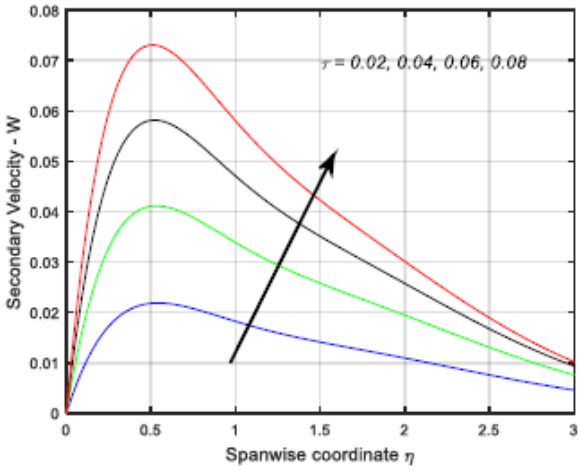

Fig 19: Influence of time on the secondary velocity.

5. ACKNOWLEDGEMENTS

Authors are thankful for the comments and suggestions of the referees, which have led to improvement of this paper.

Nomenclature

u	fluid velocity in $x-$ direction
w	fluid velocity in $z-$ direction
g	acceleration due to gravity
t	dimensional time
K_1	permeability of porous medium
B_o	uniform magnetic field
T	fluid temperature
m	hall current parameter
k_T	thermal conductivity
C	species concentration
c_p	specific heat at constant pressure
D_M	chemical molecular diffusive
D_T	thermal diffusivity
q_r	radiating flux vector
T_w	temperature of the wall
C_w	concentration of the wall
T_∞	fluid temperature in the free stream
C_∞	species concentration in the free stream
a^*	mean absorption coefficient
N	buoyancy parameter
Pr	Prandtl number
T_M	mean temperature
R	radiation parameter
K^2	rotation parameter
M	magnetic parameter
Sc	Schmidt number
K	permeability parameter
Sr	Soret number
u_o	characteristic velocity
U	primary velocity
W	secondary velocity

Greek Symbols

ρ	fluid density
β_T	coefficient of thermal expansion
β_C	coefficient of concentration expansion
Ω	uniform angular velocity
σ	electrical conductivity
ν	kinematic coefficient of viscosity
ω_e	cyclotron frequency
τ_e	electron collision time
σ^*	Stefan- Boltzmann constant
θ	non dimensional temperature
ϕ	non dimensional concentration

6. REFERENCES

1. *Seth GS, Hussain M, Sarkar S. Effects of hall current and rotation on unsteady MHD natural convection flow with heat and mass transfer past an impulsively moving vertical plate in the presence of radiation and chemical reaction, Bulgarian Chemical Communications. 2014; 46: 704–718.*
2. *Venkateswarlu M, Vasu Babu R, Mohiddin Shaw SK. Dufour and heat source effects on radiative MHD slip flow of a viscous fluid in a parallel porous plate channel in presence of chemical reaction, J. Korean Soc. Ind. Appl. Math, 2017; 21(4): 245 – 275.*
3. *Reddy MG. Influence of thermal radiation, viscous dissipation and hall current on MHD convection flow over a stretched vertical flat plate, Ain Shams Engineering Journal. 2014; 5:169 – 175.*
4. *Venkateswarlu M, Makinde OD, Lakshmi DV. Influence of thermal radiation and heat generation on steady hydromagnetic flow in a vertical micro-porous-channel in presence of suction/injection, Journal of Nanofluids. 2019; 8(5): 1010 – 1019.*
5. *Vieru D, Fetecau C, Nigar N. Magnetohydrodynamic natural convection flow with Newtonian heating and mass diffusion over an infinite plate that applies shear stress to a viscous fluid, Zeitschrift für Naturforschung A. 2014; 69a: 714 – 724.*
6. *Venkateswarlu M, Upender Reddy G, Venkata Lakshmi D. Influence of Hall current and heat source on MHD flow of a rotating fluid in a parallel porous plate channel, J. Korean Soc. Ind. Appl. Math. 2018; 22(4): 217 – 239.*
7. *Uddin Z, Kumar M, Harmand S. Influence of thermal radiation and heat generation/absorption on MHD heat transfer flow of a micropolar fluid past a wedge considering hall and ion slip currents, Thermal Science. 2014; 18: 489 – 502.*
8. *Venkateswarlu M, Phani Kumar M. Soret and heat source effects on MHD flow of a viscous fluid in a parallel porous plate channel in presence of slip condition, U. P. B. Sci. Bull., Series D: Mechanical Engineering. 2017; 79: 171 – 186.*
9. *Takhar HS, Roy S, Nath G. Unsteady free convection flow over an infinite vertical porous plate due to the combined effects of thermal and mass diffusion, magnetic field and Hall currents, Heat Mass Transfer. 2003; 39: 825–34.*
10. *Malapati V, Dasari VL. Soret and chemical reaction effects on the radiative MHD flow from an infinite vertical plate, J. Korean Soc. Ind. Appl. Math. 2017; 21: 39 – 61.*
11. *Seth GS, Mahato GK, Sarkar S. Effects of Hall current and rotation on MHD natural convection flow past an impulsively moving vertical plate with ramped temperature in the presence of thermal diffusion with heat absorption, Int. J Energy Tech. 2013; 5: 1–12.*
12. *Venkateswarlu M, Makinde OD. Unsteady MHD slip flow with radiative heat and mass transfer over an inclined plate embedded in a porous medium, Defect and Diffusion Forum. 2018; 384: 31 – 48.*
13. *Sattar MA. Unsteady hydromagnetic free convection flow with Hall current mass transfer and variable suction through a porous medium near an infinite vertical porous plate with constant heat flux, Int. J. Energy Research. 1993; 17: 1 – 5.*
14. *Venkateswarlu M, Venkata Lakshmi D, Makinde OD. Thermodynamic analysis of Hall current and Soret number on hydromagnetic couette flow in a rotating system with a convective boundary condition, Heat Transfer Research. 2020; 51: 83–101.*
15. *Seth GS, Kumbhakar B, Sharma R. Unsteady hydromagnetic natural convection flow of a heat absorbing fluid within a rotating vertical channel in porous medium with Hall effects, J. Appl. Fluid Mech. 2015; 8: 767 – 779.*
16. *Venkateswarlu M, Prameela M, Makinde OD. Influence of heat generation and viscous dissipation on hydromagnetic fully developed natural convection flow in a vertical micro–channel, Journal of Nanofluids. 2019; 8: 506 – 1516.*
17. *Venkateswarlu M, Bhaskar P, Venkata Lakshmi D. Soret and Dufour effects on radiative hydromagnetic flow of a chemically reacting fluid over an exponentially accelerated inclined porous plate in presence of heat absorption and viscous dissipation, J. Korean Soc. Ind. Appl. Math. 2019; 23(3): 157 – 178.*
18. *Ahmed N. Soret and Radiation effects on transient MHD free convection from an impulsively started infinite vertical plate, Journal of Heat Transfer. 2012; 134: 062701 – 1 – 9.*

ISSN: 2632-9417

Parameter Estimation of Inverted Exponential Distribution Via Bayesian Approach

Arun Kumar Rao[1], Himanshu Pandey[2]
[1-2] Department of Mathematics & Statistics, DDU Gorakhpur University, Gorakhpur, India

ABSTRACT

In this paper, the inverted exponential distribution is considered for Bayesian analysis. The expressions for Bayes estimators of the parameter have been derived under squared error, precautionary, entropy, K-loss, and Al-Bayyati's loss functions by using quasi and gamma priors.

Keywords: Inverted exponential distribution, Bayesian method, quasi and gamma priors, squared error, precautionary, entropy, K-loss, and Al-Bayyati's loss functions.

INTRODUCTION

The inverted exponential distribution is studied as a prospective life distribution (Sanku Dey [1]). The probability density function of inverted exponential distribution is given by

$$f(x;\theta)=\theta x^{-2}e^{-\theta/x} \quad ; x\geq 0,\ \theta>0. \tag{1}$$

The joint density function or likelihood function of (1) is given by

$$f(\underline{x};\theta)=\theta^{n}\left(\prod_{i=1}^{n}x_i^{-2}\right)e^{-\theta\sum_{i=1}^{n}\left(\frac{1}{x_i}\right)}. \tag{2}$$

The log likelihood function is given by

$$log\, f(\underline{x};\theta)=n log\,\theta+log\left(\prod_{i=1}^{n}x_i^{-2}\right)-\theta\sum_{i=1}^{n}\left(\frac{1}{x_i}\right) \tag{3}$$

Differentiating (3) with respect to θ and equating to zero, we get the maximum likelihood estimator of θ which is given as

$$\hat{\theta}=\frac{n}{\sum_{i=1}^{n}\left(\frac{1}{x_i}\right)}. \tag{4}$$

2. BAYESIAN METHOD OF ESTIMATION

The Bayesian inference procedures have been developed generally under squared error loss function

$$L\left(\hat{\theta},\theta\right)=\left(\hat{\theta}-\theta\right)^{2}. \tag{5}$$

The Bayes estimator under the above loss function, say, $\hat{\theta}_S$ is the posterior mean, i.e,

$$\hat{\theta}_S=E(\theta). \tag{6}$$

Zellner [2], Basu and Ebrahimi [3] have recognized that the inappropriateness of using symmetric loss function. Norstrom [4] introduced precautionary loss function is given as

$$L\left(\hat{\theta},\theta\right)=\frac{\left(\hat{\theta}-\theta\right)^2}{\hat{\theta}}. \quad (7)$$

The Bayes estimator under precautionary loss function is denoted by $\hat{\theta}_p$ and is obtained by solving the following equation

$$\hat{\theta}_P=\left[E\left(\theta^2\right)\right]^{1/2}. \quad (8)$$

In many practical situations, it appears to be more realistic to express the loss in terms of the ratio $\frac{\hat{\theta}}{\theta}$. In this case, Calabria and Pulcini [5] points out that a useful asymmetric loss function is the entropy loss

$$L(\delta)\propto\left[\delta^p-p\ log_e(\delta)-1\right]$$

where $\delta=\frac{\hat{\theta}}{\theta}$, and whose minimum occurs at $\hat{\theta}=\theta$. Also, the loss function $L(\delta)$ has been used in Dey *et al*. [6] and Dey and Liu [7], in the original form having $p=1$. Thus $L(\delta)$ can written be as

$$L(\delta)=b\left[\delta-log_e(\delta)-1\right];\ b>0. \quad (9)$$

The Bayes estimator under entropy loss function is denoted by $\hat{\theta}_E$ and is obtained by solving the following equation

$$\hat{\theta}_E=\left[E\left(\frac{1}{\theta}\right)\right]^{-1}. \quad (10)$$

Wasan [8] proposed the K-loss function which is given as

$$L\left(\hat{\theta},\theta\right)=\frac{\left(\hat{\theta}-\theta\right)^2}{\hat{\theta}\theta}. \quad (11)$$

Under K-loss function the Bayes estimator of θ is denoted by $\hat{\theta}_K$ and is obtained as

$$\hat{\theta}_K=\left[\frac{E(\theta)}{E(1/\theta)}\right]^{\frac{1}{2}}. \quad (12)$$

Al-Bayyati [9] introduced a new loss function using Weibull distribution which is given as

$$L\left(\hat{\theta},\theta\right)=\theta^c\left(\hat{\theta}-\theta\right)^2. \quad (13)$$

Under Al-Bayyati's loss function the Bayes estimator of θ is denoted by $\hat{\theta}_{Al}$ and is obtained as

$$\hat{\theta}_{Al}=\frac{E\left(\theta^{c+1}\right)}{E\left(\theta^c\right)}. \quad (14)$$

Let us consider two prior distributions of θ to obtain the Bayes estimators.

(i) Quasi-prior: For the situation where we have no prior information about the parameter θ, we may use the quasi density as given by

$$g_1(\theta)=\frac{1}{\theta^d}\ ;\ \theta>0,\ d\geq 0, \quad (15)$$

where $d = 0$ leads to a diffuse prior and $d = 1$, a non-informative prior.
(ii) Gamma prior: Generally, the gamma density is used as prior distribution of the parameter θ given by

$$g_2(\theta) = \frac{\beta^{\alpha}}{\Gamma(\alpha)} \theta^{\alpha-1} e^{-\beta\theta} \; ; \; \theta > 0. \tag{16}$$

3. Posterior density under $g_1(\theta)$

The posterior density of θ under $g_1(\theta)$, on using (2), is given by

$$f(\theta/\underline{x}) = \frac{\theta^n \left(\prod_{i=1}^{n} x_i^{-2} \right) e^{-\theta \sum_{i=1}^{n} \left(\frac{1}{x_i} \right)} \theta^{-d}}{\int_0^{\infty} \theta^n \left(\prod_{i=1}^{n} x_i^{-2} \right) e^{-\theta \sum_{i=1}^{n} \left(\frac{1}{x_i} \right)} \theta^{-d} d\theta}$$

$$= \frac{\theta^{n-d} \; e^{-\theta \sum_{i=1}^{n} \left(\frac{1}{x_i} \right)}}{\int_0^{\infty} \theta^{n-d} \; e^{-\theta \sum_{i=1}^{n} \left(\frac{1}{x_i} \right)} d\theta}$$

$$= \frac{\left(\sum_{i=1}^{n} \left(\frac{1}{x_i} \right) \right)^{n-d+1}}{\Gamma(n-d+1)} \; \theta^{n-d} \; e^{-\theta \sum_{i=1}^{n} \left(\frac{1}{x_i} \right)} \tag{17}$$

Theorem 1. On using (17), we have

$$E(\theta^c) = \frac{\Gamma(n-d+c+1)}{\Gamma(n-d+1)} \left(\sum_{i=1}^{n} \left(\frac{1}{x_i} \right) \right)^{-c} . \tag{18}$$

Proof. By definition,

$$E(\theta^c) = \int \theta^c f(\theta/\underline{x}) d\theta$$

$$= \frac{\left(\sum_{i=1}^{n} \left(\frac{1}{x_i} \right) \right)^{n+d-1}}{\Gamma(n+d-1)} \int_0^{\infty} \theta^{-(n-d+c)} \; e^{-\theta \sum_{i=1}^{n} \left(\frac{1}{x_i} \right)} d\theta$$

$$= \frac{\left(\sum_{i=1}^{n}\left(\frac{1}{x_i}\right)\right)^{n-d+1}}{\Gamma(n-d+1)} \frac{\Gamma(n-d+c+1)}{\left(\sum_{i=1}^{n}\left(\frac{1}{x_i}\right)\right)^{n-d+c+1}}$$

$$= \frac{\Gamma(n-d+c+1)}{\Gamma(n-d+1)}\left(\sum_{i=1}^{n}\left(\frac{1}{x_i}\right)\right)^{-c}.$$

From equation (18), for $c=1$, we have

$$E(\theta) = (n-d+1)\left[\sum_{i=1}^{n}\left(\frac{1}{x_i}\right)\right]^{-1}. \tag{19}$$

From equation (18), for $c=2$, we have

$$E(\theta^2) = \left[(n-d+2)(n-d+1)\right]\left[\sum_{i=1}^{n}\left(\frac{1}{x_i}\right)\right]^{-2}. \tag{20}$$

From equation (18), for $c=-1$, we have

$$E\left(\frac{1}{\theta}\right) = \frac{1}{(n-d)}\sum_{i=1}^{n}\left(\frac{1}{x_i}\right). \tag{21}$$

From equation (18), for $c=c+1$, we have

$$E(\theta^{c+1}) = \frac{\Gamma(n-d+c+2)}{\Gamma(n-d+1)}\left(\sum_{i=1}^{n}\left(\frac{1}{x_i}\right)\right)^{-(c+1)}. \tag{22}$$

4. Bayes Estimators under $g_1(\theta)$

From equation (6), on using (19), the Bayes estimator of θ under squared error loss function is given by

$$\hat{\theta}_S = (n-d+1)\left[\sum_{i=1}^{n}\left(\frac{1}{x_i}\right)\right]^{-1}. \tag{23}$$

From equation (8), on using (20), the Bayes estimator of θ under precautionary loss function is given by

$$\hat{\theta}_P = \left[(n-d+2)(n-d+1)\right]^{\frac{1}{2}}\left(\sum_{i=1}^{n}\left(\frac{1}{x_i}\right)\right)^{-1}. \tag{24}$$

From equation (10), on using (21), the Bayes estimator of θ under entropy loss function is given by

$$\hat{\theta}_E = (n-d)\left(\sum_{i=1}^{n}\left(\frac{1}{x_i}\right)\right)^{-1}. \tag{25}$$

From equation (12), on using (19) and (21), the Bayes estimator of θ under K-loss function is given by

$$\hat{\theta}_K = \left[(n-d+1)(n-d)\right]^{\frac{1}{2}} \left(\sum_{i=1}^{n} \left(\frac{1}{x_i} \right) \right)^{-1} . \tag{26}$$

From equation (14), on using (18) and (22), the Bayes estimator of θ under Al-Bayyati's loss function is given by

$$\hat{\theta}_{Al} = (n-d+c+1) \left(\sum_{i=1}^{n} \left(\frac{1}{x_i} \right) \right)^{-1} . \tag{27}$$

5. Posterior density under $g_2(\theta)$

Under $g_2(\theta)$, the posterior density of θ, using equation (2), is obtained as

$$f(\theta/\underline{x}) = \frac{\theta^n \left(\prod_{i=1}^{n} x_i^{-2} \right) e^{-\theta \sum_{i=1}^{n} \left(\frac{1}{x_i} \right)} \frac{\beta^\alpha}{\Gamma(\alpha)} \theta^{\alpha-1} e^{-\beta\theta}}{\int_0^\infty \theta^n \left(\prod_{i=1}^{n} x_i^{-2} \right) e^{-\theta \sum_{i=1}^{n} \left(\frac{1}{x_i} \right)} \frac{\beta^\alpha}{\Gamma(\alpha)} \theta^{\alpha-1} e^{-\beta\theta} d\theta}$$

$$= \frac{\theta^{n+\alpha-1} e^{-\left(\beta + \sum_{i=1}^{n} \left(\frac{1}{x_i} \right) \right)\theta}}{\int_0^\infty \theta^{n+\alpha-1} e^{-\left(\beta + \sum_{i=1}^{n} \left(\frac{1}{x_i} \right) \right)\theta} d\theta}$$

$$= \frac{\theta^{n+\alpha-1} e^{-\left(\beta + \sum_{i=1}^{n} \left(\frac{1}{x_i} \right) \right)\theta}}{\Gamma(n+\alpha) \Big/ \left(\beta + \sum_{i=1}^{n} \left(\frac{1}{x_i} \right) \right)^{n+\alpha}}$$

$$= \frac{\left(\beta + \sum_{i=1}^{n} \left(\frac{1}{x_i} \right) \right)^{n+\alpha}}{\Gamma(n+\alpha)} \theta^{n+\alpha-1} e^{-\left(\beta + \sum_{i=1}^{n} \left(\frac{1}{x_i} \right) \right)\theta} \tag{28}$$

Theorem 2. On using (28), we have

$$E(\theta^c) = \frac{\Gamma(n+\alpha+c)}{\Gamma(n+\alpha)} \left(\beta + \sum_{i=1}^{n} \left(\frac{1}{x_i} \right) \right)^{-c} . \tag{29}$$

Proof. By definition,

$$E(\theta^c) = \int \theta^c f(\theta/\underline{x}) d\theta$$

$$= \frac{\left(\beta + \sum_{i=1}^{n}\left(\frac{1}{x_i}\right)\right)^{n+\alpha}}{\Gamma(n+\alpha)} \int_0^{\infty} \theta^{n+\alpha+c-1} e^{-\left(\beta+\sum_{i=1}^{n}\left(\frac{1}{x_i}\right)\right)\theta} d\theta$$

$$= \frac{\left(\beta + \sum_{i=1}^{n}\left(\frac{1}{x_i}\right)\right)^{n+\alpha}}{\Gamma(n+\alpha)} \frac{\Gamma(n+\alpha+c)}{\left(\beta + \sum_{i=1}^{n}\left(\frac{1}{x_i}\right)\right)^{n+\alpha+c}}$$

$$= \frac{\Gamma(n+\alpha+c)}{\Gamma(n+\alpha)} \left(\beta + \sum_{i=1}^{n}\left(\frac{1}{x_i}\right)\right)^{-c}.$$

From equation (29), for $c = 1$, we have

$$E(\theta) = (n+\alpha)\left(\beta + \sum_{i=1}^{n}\left(\frac{1}{x_i}\right)\right)^{-1}. \tag{30}$$

From equation (29), for $c = 2$, we have

$$E(\theta^2) = \left[(n+\alpha+1)(n+\alpha)\right]\left(\beta + \sum_{i=1}^{n}\left(\frac{1}{x_i}\right)\right)^{-2}. \tag{31}$$

From equation (29), for $c = -1$, we have

$$E\left(\frac{1}{\theta}\right) = \frac{1}{(n+\alpha-1)}\left(\beta + \sum_{i=1}^{n}\left(\frac{1}{x_i}\right)\right). \tag{32}$$

From equation (29), for $c = c+1$, we have

$$E(\theta^{c+1}) = \frac{\Gamma(n+\alpha+c+1)}{\Gamma(n+\alpha)}\left(\beta + \sum_{i=1}^{n}\left(\frac{1}{x_i}\right)\right)^{-(c+1)}. \tag{33}$$

6. Bayes Estimators under g2 (θ)

From equation (6), on using (30), the Bayes estimator of θ under squared error loss function is given by

$$\hat{\theta}_S = (n+\alpha)\left(\beta + \sum_{i=1}^{n}\left(\frac{1}{x_i}\right)\right)^{-1}. \quad (34)$$

From equation (8), on using (31), the Bayes estimator of θ under precautionary loss function is given by

$$\hat{\theta}_P = \left[(n+\alpha+1)(n+\alpha)\right]^{\frac{1}{2}}\left(\beta + \sum_{i=1}^{n}\left(\frac{1}{x_i}\right)\right)^{-1}. \quad (35)$$

From equation (10), on using (32), the Bayes estimator of θ under entropy loss function is given by

$$\hat{\theta}_E = (n+\alpha+1)\left(\beta + \sum_{i=1}^{n}\left(\frac{1}{x_i}\right)\right)^{-1}. \quad (36)$$

From equation (12), on using (30) and (32), the Bayes estimator of θ under K-loss function is given by

$$\hat{\theta}_K = \left[(n+\alpha)(n+\alpha-1)\right]^{\frac{1}{2}}\left(\beta + \sum_{i=1}^{n}\left(\frac{1}{x_i}\right)\right)^{-1}. \quad (37)$$

From equation (14), on using (29) and (33), the Bayes estimator of θ under Al-Bayyati's loss function is given by

$$\hat{\theta}_{Al} = (n+\alpha+c)\left(\beta + \sum_{i=1}^{n}\left(\frac{1}{x_i}\right)\right)^{-1}. \quad (38)$$

CONCLUSION

In this paper, we have obtained a number of estimators of parameter of inverted exponential distribution. In equation (4) we have obtained the maximum likelihood estimator of the parameter. In equation (23), (24), (25), (26) and (27) we have obtained the Bayes estimators under different loss functions using quasi prior. In equation (34), (35), (36), (37) and (38) we have obtained the Bayes estimators under different loss functions using gamma prior. In the above equation, it is clear that the Bayes estimators depend upon the parameters of the prior distribution.

REFERENCES

1. *Sanku Dey. Inverted exponential distribution as a life distribution model from a Bayesian viewpoint. Data Science Journal, 2007, 6.*
2. *Zellner A. Bayesian estimation and prediction using asymmetric loss functions. Jour. Amer. Stat. Assoc. 1986; 91:446-451.*
3. *Basu AP, Ebrahimi N. Bayesian approach to life testing and reliability estimation using asymmetric loss function. Jour. Stat. Plann. Infer. 1991; 29:21-31.*
4. *Norstrom JG. The use of precautionary loss functions in Risk Analysis. IEEE Trans. Reliab. 1996; 45(3):400-403.*
5. *Calabria R, Pulcini G. Point estimation under asymmetric loss functions for left truncated exponential samples. Comm. Statist. Theory & Methods. 1994; 25(3):585-600.*
6. *DK Dey, Ghosh M, Srinivasan C. Simultaneous estimation of parameters under entropy loss. Jour. Statist. Plan. And infer, 1987, 347-363.*
7. *Dey DK, Pei-San Liao Liu. On comparison of estimators in a generalized life. Model. Microelectron. Reliab. 1992; 32(1/2):207- 221.*
8. *Wasan MT. Parametric Estimation". New York: Mcgraw-Hill, 1970.*
9. *Al-Bayyati. Comparing methods of estimating Weibull failure models using simulation". Ph.D. Thesis, College of Administration and Economics, Baghdad University, Iraq, 2002.*

ISSN: 2632-9417

A Study of Formation and Evolution of Black Hole

Neeraj Kumar Mishra[1*], Priyanka Vaidya[2]

[1] Department of Physics, National Institute of Technology, Patna, Bihar, India

[2] Department of Physics, Magadh University, Bodh Gaya, Bihar, India

ABSTRACT

Objects whose gravitational fields are too strong for light to escape were first considered in the 18th century by John Michell and Pierre-Simon Laplace. The first modern solution of general relativity that would characterize a black hole was found by Karl Schwarzschild in 1916, although its interpretation as a region of space from which nothing can escape was first published by David Finkelstein in 1958. Black holes were long considered a mathematical curiosity; it was not until the 1960s that theoretical work showed they were a generic prediction of general relativity. The discovery of neutron stars by Jocelyn Bell Burnell in 1967 sparked interest in gravitationally collapsed compact objects as a possible astrophysical reality. A black hole can be formed by the death of a massive star. When such a star has exhausted the internal thermonuclear fuels in its core at the end of its life, the core becomes unstable and gravitationally collapses inward upon itself, and the star's outer layers are blown away.

Keywords: Black Hole, General Relativity, Chandrashekhar Limit, Schwarzschild radius

INTRODUCTION

A black hole is a region of space-time where gravity is so strong that nothing (no particles or even electromagnetic radiation such as light) can escape from it. Marcia Bartusiak traces the term "black hole" to physicist Robert H. Dicke who in the early 1960s reportedly compared the phenomenon to the Black Hole of Calcutta, notorious as a prison where people entered but never left alive.

The idea of a body so massive that even light could not escape was briefly proposed by astronomical pioneer and English clergyman John Michell in a letter published in November 1784. John Michell used the term "dark star" for "black hole". Michell's simplistic calculations assumed such a body might have the same density as the Sun, and concluded that such a body would form when a star's diameter exceeds the Sun's by a factor of 500 and the surface escape velocity exceeds the usual speed of light. Michell correctly noted that such supermassive but non-radiating bodies might be detectable through their gravitational effects on nearby visible bodies. Scholars of the time were initially excited by the proposal that giant but invisible stars might be hiding in plain view, but enthusiasm dampened when the wavelike nature of light became apparent in the early nineteenth century.

In 1915, Albert Einstein developed his theory of general relativity, having earlier shown that gravity does influence light's motion. Only a few months later, Karl Schwarzschild found a solution to the Einstein field equations, which describes the gravitational field of a point mass and a spherical mass. A few months after Schwarzschild, Johannes Droste independently gave the same solution for the point mass and wrote more extensively about its properties. This solution had a peculiar behaviour at what is now called the Schwarzschild radius. The nature of this surface was not quite understood at the time.

In 1924, Arthur Eddington showed that the singularity disappeared after a change of coordinates. It took until 1933 for Georges Lemaître to realize that this meant the singularity at the Schwarzschild radius was a non-physical coordinate singularity. Arthur Eddington did however comment on the possibility of a

star with mass compressed to the Schwarzschild radius in a 1926 book, noting that Einstein's theory allows us to rule out overly large densities for visible stars like Betelgeuse.

In 1931, Subrahmanyan Chandrasekhar calculated, using special relativity, that a non-rotating body of electron-degenerate matter above a certain limiting mass (now called the Chandrasekhar limit at 1.4 M ☉) has no stable solutions. His arguments were opposed by many of his contemporaries like Eddington and Lev Landau, who argued that some yet unknown mechanism would stop the collapse. They were partly correct as a white dwarf slightly more massive than the Chandrasekhar limit will collapse into a neutron star which is stable. But in 1939, Robert Oppenheimer and others predicted that neutron stars above another limit (the Tolman–Oppenheimer–Volkoff limit) would collapse further for the reasons presented by Chandrasekhar, and concluded that no law of physics was likely to intervene and stop at least some stars from collapsing to black holes. Their original calculations, based on the Pauli Exclusion Principle, gave it as 0.7 M☉ ; subsequent consideration of strong force-mediated neutron-neutron repulsion raised the estimate to approximately 1.5 M☉ to 3.0 M☉ . Observations of the neutron star merger GW170817, which is thought to have generated a black hole shortly afterward, have refined the TOV limit estimate to ~2.17 M☉ . Oppenheimer and his co-authors interpreted the singularity at the boundary of the Schwarzschild radius as indicating that this was the boundary of a bubble in which time stopped. This is a valid point of view for external observers, but not for infilling observers. Because of this property, the collapsed stars were called "frozen stars", because an outside observer would see the surface of the star frozen in time at the instant where its collapse takes it to the Schwarzschild radius.

In 1958, David Finkelstein identified the Schwarzschild surface as an event horizon, "a perfect unidirectional membrane: causal influences can cross it in only one direction". This did not strictly contradict Oppenheimer's results, but extended them to include the point of view of infalling observers. Finkelstein's solution extended the Schwarzschild solution for the future of observers falling into a black hole. A complete extension had already been found by Martin Kruskal, who was urged to publish it. These results came at the beginning of the golden age of general relativity, which was marked by general relativity and black holes becoming mainstream subjects of research. This process was helped by the discovery of pulsars by Jocelyn Bell Burnell in 1967, which, by 1969, were shown to be rapidly rotating neutron stars. Until that time, neutron stars, like black holes, were regarded as just theoretical curiosities; but the discovery of pulsars showed their physical relevance and spurred a further interest in all types of compact objects that might be formed by gravitational collapse. In this period more general black hole solutions were found.

In 1963, Roy Kerr found the exact solution for a rotating black hole. Two years later, Ezra Newman found the axisymmetric solution for a black hole that is both rotating and electrically charged. Through the work of Werner Israel, Brandon Carter, and David Robinson the no-hair theorem emerged, stating that a stationary black hole solution is completely described by the three parameters of the Kerr–Newman metric: mass, angular momentum, and electric charge. Work by James Bardeen, Jacob Bekenstein, Carter, and Hawking in the early 1970s led to the formulation of black hole thermodynamics. These laws describe the behavior of a black hole in close analogy to the laws of thermodynamics by relating mass to energy, area to entropy, and surface gravity to temperature. The analogy was completed when Hawking, in 1974, showed that quantum field theory implies that black holes should radiate like a black body with a temperature proportional to the surface gravity of the black hole, predicting the effect now known as Hawking radiation.

On 11 February 2016, the LIGO Scientific Collaboration and the Virgo collaboration announced the first direct detection of gravitational waves, which also represented the first observation of a black hole merger. On 10 April 2019, the first direct image of a black hole and its vicinity was published, following observations made by the Event Horizon Telescope in 2017 of the supermassive black hole in Messier 87's galactic centre.

At first, it was suspected that the strange features of the black hole solutions were pathological artifacts from the symmetry conditions imposed, and that the singularities would not appear in generic situations. This view was held in particular by Vladimir Belinsky, Isaak Khalatnikov, and Evgeny Lifshitz, who tried to prove that no singularities appear in generic solutions. However, in the late 1960s Roger Penrose and Stephen Hawking used global techniques to prove that singularities appear generically. For this work, Penrose received half of the 2020 Nobel Prize in Physics.

FORMATION OF BLACK HOLE

Given the bizarre character of black holes, it was long questioned whether such objects could actually exist in nature or whether they were merely pathological solutions to Einstein's equations. Einstein himself wrongly thought black holes would not form, because he held that the angular momentum of collapsing particles would stabilize their motion at some radius. This led the general relativity community to dismiss all results to the contrary for many years. However, a minority of relativists continued to contend that black holes were physical objects, and by the end of the 1960s, they had persuaded the majority of researchers in the field that there is no obstacle to the formation of an event horizon.

Penrose demonstrated that once an event horizon forms, general relativity without quantum mechanics requires that a singularity will form within. Shortly afterwards, Hawking showed that many cosmological solutions that describe the Big Bang have singularities without scalar fields or other exotic matter. The Kerr solution, the no-hair theorem, and the laws of black hole thermodynamics showed that the physical properties of black holes were simple and comprehensible, making them respectable subjects for research. Conventional black holes are formed by gravitational collapse of heavy objects such as stars, but they can also in theory be formed by other processes.

GRAVITATIONAL COLLAPSE

Gravitational collapse occurs when an object's internal pressure is insufficient to resist the object's own gravity. For stars this usually occurs either because a star has too little fuel left to maintain its temperature through stellar nucleosynthesis or because a star that would have been stable receives extra matter in a way that does not raise its core temperature. In either case the star's temperature is no longer high enough to prevent it from collapsing under its own weight. The collapse may be stopped by the degeneracy pressure of the star's constituents, allowing the condensation of matter into an exotic denser state. The result is one of the various types of compact star. Which type forms depends on the mass of the remnant of the original star left if the outer layers have been blown away (for example, in a Type II supernova). The mass of the remnant, the collapsed object that survives the explosion, can be substantially less than that of the original star. Remnants exceeding 5 M☉ are produced by stars that were over 20 M☉ before the collapse.

If the mass of the remnant exceeds about 3-4 M☉ (the Tolman–Oppenheimer–Volkoff limit) either because the original star was very heavy or because the remnant collected additional mass through

accretion of matter, even the degeneracy pressure of neutrons is insufficient to stop the collapse. No known mechanism (except possibly quark degeneracy pressure, see quark star) is powerful enough to stop the implosion and the object will inevitably collapse to form a black hole.

The gravitational collapse of heavy stars is assumed to be responsible for the formation of stellar mass black holes. Star formation in the early universe may have resulted in very massive stars, which upon their collapse would have produced black holes of up to 103 M⊙. These black holes could be the seeds of the supermassive black holes found in the centers of most galaxies. It has further been suggested that massive black holes with typical masses of ~105 M⊙ could have formed from the direct collapse of gas clouds in the young universe. These massive objects have been proposed as the seeds that eventually formed the earliest quasars observed already at redshift. While most of the energy released during gravitational collapse is emitted very quickly, an outside observer does not actually see the end of this process. Even though the collapse takes a finite amount of time from the reference frame of infalling matter, a distant observer would see the infalling material slow and halt just above the event horizon, due to gravitational time dilation. Light from the collapsing material takes longer and longer to reach the observer, with the light emitted just before the event horizon forms delayed an infinite amount of time. Thus the external observer never sees the formation of the event horizon; instead, the collapsing material seems to become dimmer and increasingly red-shifted, eventually fading away.

Gravitational collapse requires great density. In the current epoch of the universe these high densities are found only in stars, but in the early universe shortly after the Big Bang densities were much greater, possibly allowing for the creation of black holes. High density alone is not enough to allow black hole formation since a uniform mass distribution will not allow the mass to bunch up. In order for primordial black holes to have formed in such a dense medium, there must have been initial density perturbations that could then grow under their own gravity. Different models for the early universe vary widely in their predictions of the scale of these fluctuations. Various models predict the creation of primordial black holes ranging in size from Planck mass to hundreds of thousands of solar masses.

Despite the early universe being extremely dense—far denser than is usually required to form a black hole-it did not re-collapse into a black hole during the Big Bang. Models for gravitational collapse of objects of relatively constant size, such as stars, do not necessarily apply in the same way to rapidly expanding space such as the Big Bang.

HIGH-ENERGY COLLISIONS

Gravitational collapse is not the only process that could create black holes. In principle, black holes could be formed in high-energy collisions that achieve sufficient density. As of 2002, no such events have been detected, either directly or indirectly as a deficiency of the mass balance in particle accelerator experiments. This suggests that there must be a lower limit for the mass of black holes. Theoretically, this boundary is expected to lie around the Planck mass ($m_P=\sqrt{\hbar c/G} \approx 1.2\times10^{19}$ GeV/c2 $\approx 2.2\times10^{-8}$ kg), where quantum effects are expected to invalidate the predictions of general relativity. This would put the creation of black holes firmly out of reach of any high-energy process occurring on or near the Earth. However, certain developments in quantum gravity suggest that the minimum black hole mass could be much lower as low as 1 TeV/c2. This would make it conceivable for micro black holes to be created in the high-energy collisions that occur when cosmic rays hit the Earth's atmosphere or possibly in the Large Hadron Collider at CERN. These theories are very speculative and the creation of black holes in these processes is deemed unlikely by many specialists. Even if micro black holes could be formed, it is expected that they would evaporate in about 10^{-25} seconds, posing no threat to the Earth.

GROWTH OF BLACK HOLE

Once a black hole has formed, it can continue to grow by absorbing additional matter. Any black hole will continually absorb gas and interstellar dust from its surroundings. This is the primary process through which supermassive black holes seem to have grown. A similar process has been suggested for the formation of intermediate-mass black holes found in globular clusters. Black holes can also merge with other objects such as stars or even other black holes. This is thought to have been important, especially in the early growth of supermassive black holes, which could have formed from the aggregation of many smaller objects. The process has also been proposed as the origin of some intermediate-mass black holes.

EVAPORATION AND SHRINKAGE OF BLACK HOLE

In 1974, Hawking predicted that black holes are not entirely black but emit small amounts of thermal radiation at a temperature $\hbar$ c3/(8 π G M kB); this effect has become known as Hawking radiation. By applying quantum field theory to a static black hole background, he determined that a black hole should emit particles that display a perfect black body spectrum. Since Hawking's publication, many others have verified the result through various approaches. If Hawking's theory of black hole radiation is correct, then black holes are expected to shrink and evaporate over time as they lose mass by the emission of photons and other particles. The temperature of this thermal spectrum (Hawking temperature) is proportional to the surface gravity of the black hole, which, for a Schwarzschild black hole, is inversely proportional to the mass. Hence, large black holes emit less radiation than small black holes.

A stellar black hole of 1 M$\odot$ has a Hawking temperature of 62 nanokelvins. This is far less than the 2.7 K temperature of the cosmic microwave background radiation. Stellar-mass or larger black holes receive more mass from the cosmic microwave background than they emit through Hawking radiation and thus will grow instead of shrinking. To have a Hawking temperature larger than 2.7 K (and be able to evaporate), a black hole would need a mass less than the Moon. Such a black hole would have a diameter of less than a tenth of a millimeter.

If a black hole is very small, the radiation effects are expected to become very strong. A black hole with the mass of a car would have a diameter of about 10−24 m and take a nanosecond to evaporate, during which time it would briefly have a luminosity of more than 200 times that of the Sun. Lower-mass black holes are expected to evaporate even faster; for example, a black hole of mass 1 TeV/c2 would take less than 10−88 seconds to evaporate completely. For such a small black hole, quantum gravitation effects are expected to play an important role and could hypothetically make such a small black hole stable, although current developments in quantum gravity do not indicate this is the case.

The Hawking radiation for an astrophysical black hole is predicted to be very weak and would thus be exceedingly difficult to detect from Earth. A possible exception, however, is the burst of gamma rays emitted in the last stage of the evaporation of primordial black holes. Searches for such flashes have proven unsuccessful and provide stringent limits on the possibility of existence of low mass primordial black holes. NASA's Fermi Gamma-ray Space Telescope launched in 2008 will continue the search for these flashes.

If black holes evaporate via Hawking radiation, a solar mass black hole will evaporate (beginning once the temperature of the cosmic microwave background drops below that of the black hole) over a period

of 1064 years. A super massive black hole with a mass of 1011 (100 billion) M☉ will evaporate in around 2×10100 years. Some monster black holes in the universe are predicted to continue to grow up to perhaps 1014 M☉ during the collapse of super clusters of galaxies. Even these would evaporate over a timescale of up to 10106 years.

CONCLUSION

The theory of general relativity predicts that a sufficiently compact mass can deform spacetime to form a black hole. The boundary of the region from which no escape is possible is called the event horizon. Although the event horizon has an enormous effect on the fate and circumstances of an object crossing it, according to general relativity it has no locally detectable features. In many ways, a black hole acts like an ideal black body, as it reflects no light. Moreover, quantum field theory in curved space-time predicts that event horizons emit Hawking radiation, with the same spectrum as a black body of a temperature inversely proportional to its mass. This temperature is on the order of billionths of a kelvin for black holes of stellar mass, making it essentially impossible to observe.

Black holes of stellar mass are expected to form when very massive stars collapse at the end of their life cycle. After a black hole has formed, it can continue to grow by absorbing mass from its surroundings. By absorbing other stars and merging with other black holes, supermassive black holes of millions of solar masses (M☉) may form. There is consensus that supermassive black holes exist in the centers of most galaxies.

The presence of a black hole can be inferred through its interaction with other matter and with electromagnetic radiation such as visible light. Matter that falls onto a black hole can form an external accretion disk heated by friction, forming quasars, some of the brightest objects in the universe. Stars passing too close to a supermassive black hole can be shred into streamers that shine very brightly before being "swallowed." If there are other stars orbiting a black hole, their orbits can be used to determine the black hole's mass and location. Such observations can be used to exclude possible alternatives such as neutron stars. In this way, astronomers have identified numerous stellar black hole candidates in binary systems, and established that the radio source known as Sagittarius A*, at the core of the Milky Way galaxy, contains a supermassive black hole of about 4.3 million solar masses.

REFERENCES

1. *Wald RM. Gravitational Collapse and Cosmic Censorship. Black Holes, Gravitational Radiation and the Universe. Springer, 1997, 69-86.*
2. *Schutz Bernard F. Gravity from the ground up. Cambridge University Press, 2003, 110.*
3. *Davies PCW Thermodynamics of Black Holes (PDF). Reports on Progress in Physics. 1978; 41(8):1313-1355.*
4. *Montgomery Colin, Orchiston Wayne, Whittingham Ian. Michell, Laplace and the origin of the black hole concept. Journal of Astronomical History and Heritage. 2009; 12(2):90-96.*
5. *Clery D. Black holes caught in the act of swallowing stars". Science. 2020; 367(6477):495.*
6. *Abbott BP. Observation of Gravitational Waves from a Binary Black Hole Merger. Phys. Rev. Lett. 2016; 116:(6)*
7. *Bouman Katherine L, Johnson Michael D, Zoran Daniel Fish, Vincent L, Doeleman Sheperd S, Freeman William T. Computational Imaging for VLBI Image Reconstruction. 2016 IEEE Conference on Computer Vision and Pattern Recognition (CVPR), 2016, 913-922.*
8. *Oldham LJ, Auger MW. Galaxy structure from multiple tracers-II. M87 from parsec to megaparsec scales". Monthly Notices of the Royal Astronomical Society. 2016; 457(1):421-439.*
9. *Slayter Elizabeth M, Slayter Henry S. Light and Electron Microscopy. Cambridge University Press, 1992. ISBN 978-0-521-33948-3.*
10. *Droste J. On the field of a single centre in Einstein's theory of gravitation, and the motion of a particle in that field" (PDF). Proceedings Royal Academy Amsterdam. 1917; 19(1):197-215.*

11. *Kox AJ. General Relativity in the Netherlands: 1915-1920. Studies in the history of general relativity. Birkhäuser, 1992, 41.*
12. *Hooft G. Introduction to the Theory of Black Holes" (PDF). Institute for Theoretical Physics / Spinoza Institute, 2009, 47-48.*
13. *Eddington Arthur. The Internal Constitution of the Stars. Science. Cambridge University Press, 1926; 52:233-40.*
14. *Thorne Kip S, Hawking Stephen. Black Holes and Time Warps: Einstein's Outrageous Legacy. W. W. Norton & Company, 1994; 134-135.*
15. *Venkataraman G. Chandrasekhar and his limit. Universities Press, 1992, 89.*
16. *Detweiler S. Resource letter BH-1: Black holes". American Journal of Physics. 1981; 49(5):394-400.*
17. *Harpaz A. Stellar evolution. A K Peters, 1994, 105.*
18. *Oppenheimer JR, Volkoff GM. On Massive Neutron Cores. Physical Review. 1939; 55(4):374-381.*
19. *Bombaci I. The Maximum Mass of a Neutron Star. Astronomy and Astrophysics. 1996; 305:871-877.*
20. *Ferguson Kitty. Black Holes in Space-Time. Watts Franklin, 1991*
21. *Hawking Stephen. A Brief History of Time. Bantam Books, Inc, 1988.*
22. *Hawking Stephen, Penrose Roger. The Nature of Space and Time. Princeton University Press, 1996.*
23. *Melia Fulvio. The Black Hole at the Center of Our Galaxy. Princeton U Press, 2003.*
24. *Melia Fulvio. The Edge of Infinity. Supermassive Black Holes in the Universe. Cambridge U Press, 2003.*
25. *Pickover Clifford. Black Holes: A Traveler's Guide. Wiley, John & Sons, Inc, 1998.*
26. *Thorne Kip S. Black Holes and Time Warps. Norton, W. W. & Company, Inc, 1994.*
27. *Susskind Leonard. The Black Hole War: My Battle with Stephen Hawking to Make the World Safe for Quantum Mechanics. Little, Brown and Company, 2008.*
28. *Wheeler J Craig. Cosmic Catastrophes (2nd ed.). Cambridge University Press, 2007.*
29. *Carroll Sean M. Spacetime and Geometry. Addison Wesley, 2004.*
30. *Carter B. Black hole equilibrium states". Black Holes.*
31. *Chandrasekhar, Subrahmanyan 1999. Mathematical Theory of Black Holes. Oxford University Press, 1973.*
32. *Frolov Valeri P, Zelnikov Andrei. Introduction to Black Hole Physics. Oxford: Oxford University Press, 2011.*
33. *Hawking SW, Ellis GFR. Large Scale Structure of space time. Cambridge University Press, 1973.*
34. *Melia Fulvio. The Galactic Supermassive Black Hole. Princeton U Press, 2007.*
35. *Misner Charles, Thorne Kip S, Wheeler John. Gravitation. WH Freeman and Company, 1973.*
36. *Taylor Edwin F, Wheeler John Archibald. Exploring Black Holes. Addison Wesley Longman, 2000.*
37. *Wald Robert M. General Relativity. University of Chicago Press, 1984.*
38. *Wald Robert M. Space, Time, and Gravity: The Theory of the Big Bang and Black Holes. University of Chicago Press, 1992.*
39. *Price Richard, Creighton Teviet. Black holes. Scholarpedia. 2008; 3(1):4277*
40. *Gallo Elena, Marolf Donald. Resource Letter BH-2: Black Holes. American Journal of Physics. 2009; 77(4):294-307*

ISSN: 2632-9417

An Evaluation of Thermal Conductivity of High-Temperature Superconductors

Neeraj Kumar Mishra[1*], Priyanka Vaidya[2]

[1] Department of Physics, National Institute of Technology, Patna, Bihar, India

[2] Department of Physics, Magadh University, Bodh Gaya, Bihar, India

ABSTRACT

This paper deals with the transport properties of high temperature superconductors. The transport properties are temperature dependence of thermal conductivity of high Tc superconductor. We have taken two different high Tc superconductors in our studies namely $La_{2-}nSrnCuO_4$ and $YBa_2Cu_3O_{7-}\delta$. These superconductors bear transition temperature from 38K to 110K. Transport properties basically concerns with the movement of the classic carriers in the solid. In the case of superconductors the carriers are super electrons which move in the vicinity of a different excitation of the solid created by the impurity which has been dropped in the system. It was believed that as in the case of noble metal or low Tc superconductors (Tc from 1K to 24K) phonons has dominant role in different transport properties. From the investigation this has been ruled out. Phonons does play role in the high T_c superconductor only above T_c. The studies of thermal conductivities of high Tc superconductors indicate that the phonons contributions are larger near Tc and smaller far away.

Keywords: Cooper pair, electrical conductivity, Matthiessen rule, point defects, superconductor, thermal conductivity, thermal current density, Wiedemann-Franz law

1. INTRODUCTION

Thermal conductivity refers to the ability of a given material to conduct or transfer heat. It is the rate at which heat is transferred by conduction through a unit cross-section area of a material, when a temperature gradient exits perpendicular to the area.

Superconductivity is a set of physical properties observed in certain materials where electrical resistance vanishes and magnetic flux fields are expelled from the material. Any material exhibiting these properties is a Superconductor.

The scattering mechanisms involved in heat transport may be investigated through thermal conductivity measurements. In particular, measurements on high temperature superconductor $YBa_2Cu_3O_{7-}\delta$ and $La_{1.85}Sr_{0.15}CuO_4$ provide information on the scattering of photons by electrons for $T \sim T_c$.. Low temperature measurements on single crystal $YBa_2Cu_3O_{7-}\delta$ can give information on photon scattering by two level systems2 characteristic of amorphous solids.

In order to interpret the thermal conductivity experiments on the high Tc superconductor it is useful to compare their behaviour with that of conventional superconductor (i.e. superconductor which are well discussed by the Bis-mechanism of photon-mediated cooper pair formation.

2. THERMAL CONDUCTIVITY OF CONVENTIONAL SUPERCONDUCTOR

2.1 Electronic contribution to the thermal conductivity

For a superconductor, the behaviour of thermal conductivity as a function of temperature may be quite complicated. It depends for example, upon the temperature of the transition with respect to the temperatures at which various scattering mechanisms dominate the degree of physical and chemical disorder, and the purity of the material. However, if one restricts one's attention to the neigh bourhood of the superconducting transition and look for conditions between the dominant heat carrier and the form of the thermal conductivity through the transition, one can draw some single conclusions and apply them to the thermal conductivity measurements on $La_{2-}nSrnCuO_4$ and $YBa_2Cu_3O_{7-\delta}$. If electrons transport the majority of the heat, the thermal conductivity in the superconducting state is lower than the normal state conductivity for $T \sim T_c$; as electrons condense into the ground state then no longer transport entropy or heat and the thermal conductivity is correspondingly reduced.[3,4]

2.2 Phonon contribution to the thermal conductivity

When phonons transport the majority of the heat, the thermal conductivity in the superconducting state can become larger than the normal state for $T \sim T_c$; for most conventional superconductor the transition occurs in a region where phonons are scattered mainly by electrons and defects like grain boundaries, pores and point defects; below the transition electrons are effectively resumed as phonon scattering, providing an increase in the conuctivity[5]. The increase may be obscured if defect scattering dominates over electron scattering at T^c. When both electrons and phonons make comparable contribution to the thermal conductivity at T_c, either type of behaviour is possible.[6] It is useful to note that for this case when phonons transport the majority of the heat at T_c, similar behaviour is seen in both medium coupled[7] and strong coupled superconductor for both types of materials the thermal conductivity in the super conducting state in larger than the normal state conductivity for temperatures chosen to and lower than T_c. In other words, for both strong and medium coupled superconductor then is sufficient electron morrow scattering atom T_c state the thermal conductivity in the superconducting state is enhanced above the normal state conductivity as the scattering is reduced below T_c. One should be cautious, transform, in drawing conclusion about the strength of the electron phonon coupling based upon the qualitative form of the thermal conductivity at $T_c$above.

3. THERMAL CONDUCTIVITY OF HIGH TC SUPERCONDUCTOR

3.1 Non-ideal samples

Thermal conductivity measurements on high Tc superconductor have been limited mainly to ceramic samples of $YBa_2Cu_3O_{7-\delta}$ and $La_{2-}xSrxCuO_4$. Since the thermal conductivity is sensitive to the scattering mechanisms in a solid, the presence of pores and interval boundaries in ceramic materials makes the thermal conductivity data more difficult to interpret than for single crystal materials. Nonetheless, the qualitative form of the thermal conductivity as a function of temperature for the $La_{2-}nSrnCuO_4$ and $YBa_2Cu_3O_{7-\delta}$ ceramics can give us information of the scattering of phonons by electrons for $T \sim T_c$. Note that no matter what the mechanism for superconductivity is for the high Tc superconductor, electrons below T_c which have condensed with the good state cannot transport heat or scatter phonons. Only one group[9] has measured the thermal conductivity of one sample each of single crystal $YBa_2Cu_5O_{7-\delta}$ and $HoBa_2Cu_3O_{7-\delta}$. Then data provide evidence for the existence of two level symptons[10,11] in $YBa_2Cu_3O_{7-\delta}$.

3.2 Mathematical formulation used in the evaluation

One knows that the heat currents carried by conduction electron are closely related to electrical currents. An additional complication in the heat transport case is that the carriers of heat can be either charge carriers like electrons or electrically neutral phonons, whereas electrical current arises only from charge carrier transport. The transformation to the superconducting state changes the nature of the carriers of the electric current. So it is to be expected that the transport of heat will be strongly affected.[12-16]

The thermal current density J is the thermal energy per unit time crossing a unit area adjusted perpendicular to the direction of heat flow. It is a vector representing the transport of entropy density S_ϕ at the velocity $\vec{v}$,

$$\vec{J} = TS_\phi\vec{v} \qquad (1)$$

from hotter to cooler region of the material. It is proportional to the gradient of the temperature ∇T

$$q=-k\nabla T \qquad (2)$$

Where q is the local heat flux density and k is the coefficient of thermal conductivity.

In the normal state, electrical conductor is a good conductor of heat in accordance with the law of Wiedemann Franz.

$$(k/\sigma) = \frac{\pi^2}{3}(k_B/e)^2T \qquad (3)$$

Where σ is the electrical conductivity.

In the superconducting state, in contrast the heat conductivity can be much lower because cooper pairs carry no entropy and do not scatter phonon.

The principal carries of thermal energy through metals in the normal state are conduction electron and phonons. Heat conduction via each of these two channels acts independently, so that the two channels constitute parallel paths for the passage of heat. A simple model for the conduction of heat between two points A and B in the sample is to represent the two channels by parallel resistors with conductivities ke and kph for the electronic and phonons paths. The conductivities add directly as the electrical analogue of parallel resistors to give the total thermal conductivities K.

$$k(T) = k_e(T) + k_{ph}(T) \qquad (4)$$

The electronic path has an electron lattice contribution $k_{e\text{-}L}$ which is always present and an impurity term $k_{e\text{-}1}$ which becomes dominant at high defect concentrations. In like manner, the phonon path has a phonon- electron constitution $k_{ph\text{-}e}$ plus an additional contribution $k_{ph\text{-}1}$ from impurities. Since each pair of terms involves the same carriers of heat, they act in series and add as reciprocals, as in the electrical analogue can of Matthiessen rule. When the resistivity / reciprocals of conductivity) add directly.

The result is

$$\frac{1}{k_e} = \frac{1}{k_{e-L}} + \frac{1}{k_{e-1}} \qquad (5a)$$

$$\frac{1}{k_{ph}} = \frac{1}{k_{ph-e}} + \frac{1}{k_{ph-1}} \qquad (5b)$$

It is shown in standard solid state physics texts that the electronic contribution to the thermal conductivity has the form

$$K_{e\text{-}L} = \frac{1}{3} v_F I C_e \qquad (6a)$$

$$= \frac{1}{3} \gamma v_F^2 \tau T \qquad (6b)$$

When we have used electron mean free path $I = v_F \tau$ and $C_e = \gamma T$. Now we know that at low temperatures $\tau \approx T^{-3}$ and $\tau \approx T^{-1}$ at high temperatures, applying Wiedemann-Franz law gives us

$$K_{e\text{-}L} \approx \begin{cases} \frac{[constant]}{T^2} & T \ll \theta_D \\ [constant]T & T \gg \theta_D \end{cases} \qquad 7(a) \& 7(b)$$

for temperatures that are low and high respectively relative in the degree temperature θD. We know that at the lowest temperatures the electrical conductivity $\sigma(T)$ approaches a limiting value, $\sigma(T) \rightarrow \sigma_0$ arising from the impurity contribution. From this term the law of Wiedemann-Franz gives

$$k_{e\text{-}l} \rightarrow [constant]T,\ T \rightarrow 0 \qquad (8)$$

The lattice contribution to the thermal conductivity has a form which is the phonon analogue of equation 6a

$$k_{ph\text{-}L} = \frac{1}{3} v_{ph} I_{ph} C_{ph} \qquad (9)$$

The temperatures dependence of C_{ph} is more complicated than that predicted by the specific heat term, since C_{ph} increases with T whereas the phonon mean free path I_{ph} decreases with increasing temperature which not only compensates for C_{ph} but also tends to cause $k_{ph\text{-}L}$ to drop.

In pure metals the electronic contribution to the thermal conductivity tends to dominate at all temperatures. When many defects are present, as in disorganised alloys, they affect k_{ph} more than k_e and the phonon contribution can exceed that of the conduction electrons.

4. THERMAL CONDUCTIVITY BELOW T_C

Thermal conductivity involves the transport of entropy S_ϕ, super-electrons, however, do not carry entropy nor do they scatter phonons. One also know that below Tc the entropy of a superconductor drops continuously to zero, so that the thermal conductivities can be expected to decrease towards zero. In high temperature superconductor the phonon contribution to the thermal is predominant above T_c. The onset of superconductors can have the effect of first increasing the conductivity until it reaches a maximum, beyond which it decreases at lower temperature[12-18]. This increase can occur when the thermal conductivity exits from phonon electron contributing to k_{ph}. The onset of the superconducting state causes the normal electrons to condense into cooper pairs. Then no longer undergo collisions with the phonons and hence they do not participate in the phonon-electron interaction. The result is a larger mean free path I_{ph} and a larger conductivity for the uni-mediated sample below T_c[19]. Irradiating the sample produces defects that limits the mean free paths of the phonon and charge carriers and leads to decrease in the thermal conductivity and a summon of the path.

5. RESULTS AND DISCUSSION

In this paper, we have presented a method of evaluation of thermal conductivity of high Tc superconductor as a function of temperatures. The high Tc superconductor are La_2 xSr_xCuO_4 of different volumes of x (as x = 0.15, T_c= 38K and x = 0.20, T_c = 30K) and $YBa_2Cu_3O_{7-\delta}$ (T_c = 92K). We have compared our theoretical results with that of Graebner[20] and Morelli[21]. Our theoretically evaluated results are in good agreement with these workers. Our theoretical results indicate that thermal conductivities of the above superconductors increase with temperature. As it was pointed out by Uher et al[22] that phonons contribute close to 90% of the thermal conductivity in $YBa_2Cu_3O_{7-\delta}$ at T_c. Given the relatively large magnitude of Tc for $YBa_2Cu_3O_{7-\delta}$(T_c / $\theta_{Debye} \sim 0.25$). It is plausible that the transition occurs in a region where the thermal conductivity is limited mainly by phonon-phonon and carriers-phonon scattering. The enhancement of the thermal conductivity above the normal state conductivity for $T < T_c$ in $YBa_2Cu_3O_{7-\delta}$ is consistent with this interpretation. It indicates that the phonons make a major contribution to the thermal conductivity and that carrier-phonon scattering is important in limiting the phonon contribution to the thermal conductivity at T_c. On the other hand the data for $La_{2-x}SrnCuO_4$ are less conclusive. Although phonon makes major contribution[23] to the thermal conductivity at T_c, no clear enhancement is observed as for $YBa_2Cu_3O_{7-\delta}$ only a slight change in shape is noticeable at T_c. It is possible that the enhancement effect is observed in $La_{2-x}SrnCuO_4$ by scattering mechanism other than phonon-carrier scattering. The most likely scattering mechanism limiting the phonon contribution to the thermal conduct$\theta_{Debye} \sim 0.1$) are phonon defect, phonon-carrier and phonon-phonon scattering. Again defect refers to boundaries, pores and point defects. If point defects and phonon-phonon scattering overwhelmed the phonon-carrier scattering near Tc a reduction in phonon-carrier scattering below Tc will not be noticeable. The magnitude and temperature dependence of the thermal conductivity of $La_{2-x}SrxCuO_4$ and La_2CuO_4 are quite similar. Since La_2CuO_4 is a semiconductor, there should be little phonon-carrier scattering. The similarity between the $La_{2-x}SrnCuO_4$ and La_2CuO_4 data indicates, therefore, that phonon-carrier scattering is not as significant as point defects and phonon-phonon scattering near Tc in ceramic samples of $La_{2-n}SrnCuO_4$. An understanding of the scattering mechanisms which lead to the law magnitude of the thermal conductivity for $LaCuO^4$ will be important to explain[24,25] the magnitude and temperature behaviour of the thermal conductivity of $La_{2-x}SrxCuO_4$.

Table 1: An Evaluation of Thermal Conductivity k ($Wcm^{-1}K^{-1}$) as a function of temperature for $YBa_2Cu_3O_{7-\delta}$ ($T=q_2x$) k ($Wcm^{-1}K^{-1}$)

T(K)	Ohms	Graebener	Marelli
5	0.025	0.032	0.03
10	0.038	0.036	0.038
20	0.046	0.042	0.049
30	0.058	0.055	0.059
40	0.062	0.060	0.061
50	0.068	0.069	0.070
100	0.072	0.074	0.075
150	0.075	0.078	0.080
200	0.082	0.083	0.086
250	0.096	0.095	0.092

Table 2: Evaluation of Thermal conductivity k ($Wcm^{-1}K^{-1}$) as a function of temperature T for $La_{2-x}SrxCuO_4$

T(K)	k ($Wcm^{-1}K^{-1}$) X = 0.15, T_c = 38K	k ($Wcm^{-1}K^{-1}$) X = 0.2, T_c = 30K
1	0.0052	0.0046
5	0.0067	0.0058
10	0.0072	0.0070
20	0.0087	0.0084
30	0.0096	0.0095
40	0.0127	0.0120
50	0.0138	0.0136
60	0.0252	0.0246
70	0.0286	0.0273
80	0.0329	0.0308
90	0.0468	0.0458
100	0.0587	0.0553

6. CONCLUSION

Phonons does play role in the high T_c superconductor only above T_c. The studies of thermal conductivities of high T_c superconductors indicate that the phonons contributions are larger near T_c and smaller far away.

7. REFERENCES

1. Noce C, Maritato L. Phys. Rev. 1989; 1340:734.
2. Nelson DR, Seury HS. Phys, Rev. 1989; 1339:9153
3. K.H. Miller, Physica C 159, 717 (1989)
4. D.E. Morris et al, Phys. Rev. 1340, 11406 (1989)
5. T. McMullen, Phys. Rev. 1341, 877 (1990)
6. G. Kogan, Phys. Rev. 1338, 7049 (1988)
7. D.G. Hinks et al, Natum, 335, 419 (1988)
8. I. Bose, Phys. Rev. 1343, 13602 (1991)
9. P.R. Broussard, Phys. Rev. 1343, 2783 (1991)
10. B. Chakraborty, Phys. Rev. 1343, 378 (1991)
11. E.M. Chudnovsky, Phys. Rev. 1343, 7831 (1991)
12. M.P.A. Fisher, Phys. Rev. Lett. (PRL) 65, 923 (1990)
13. R. Hind, Phys. Rev 1345, 5052 (1992)
14. C.S. Hellberg and E.J. Male, Phys. Rev. 1348, 646 (1993)
15. D.R. Harshman and A.P. Mills Jr. Phys. Rev. 1345, 10684 (1992)
16. Z. Iqbal, Supercond. Rev. T, 49 (1992)
17. A.J. Millis and S. N. Coppersmith, Phys. Rev. 1343, 13770 (1991)
18. S. Sachdev, Phys. Rev. 1345, 389 (1992)
19. S. Sergunkor and M. Ausloos, Phys. Rev. 1347, 14476 (1993)
20. J.E. Graebner, B. Golding and L.C. Allen, Phys. Rev. 1334, 5696 (1986)
21. D.T. Morelli, J. Heremons and D.E. Swets, Phys. Rev. 1336, 3912 (1987)
22. C. Uher and A. B. Kaiser, Phys. Rev. 1336, 5680 (1987)
23. D. Shied M. Xu, Phys. Rev. 1349, 4548 (1991)
24. J.S. Shier and D.M. Ginsbey, Phys. Rev. 1339, 2921 (1989)
25. M. Suzuki and M. Hikita, Jpn. J. Appl. Phys. 28, 1368 (1987)

Instructions for Authors

Essentials for Publishing in this Journal

1 Submitted articles should not have been previously published or be currently under consideration for publication elsewhere.

2 Conference papers may only be submitted if the paper has been completely re-written (taken to mean more than 50%) and the author has cleared any necessary permission with the copyright owner if it has been previously copyrighted.

3 All our articles are refereed through a double-blind process.

4 All authors must declare they have read and agreed to the content of the submitted article and must sign a declaration correspond to the originality of the article.

Submission Process

All articles for this journal must be submitted using our online submissions system. http://enrichedpub.com/ . Please use the Submit Your Article link in the Author Service area.

Manuscript Guidelines

The instructions to authors about the article preparation for publication in the Manuscripts are submitted online, through the e-Ur (Electronic editing) system, developed by **Enriched Publications Pvt. Ltd**. The article should contain the abstract with keywords, introduction, body, conclusion, references and the summary in English language (without heading and subheading enumeration). The article length should not exceed 16 pages of A4 paper format.

Title

The title should be informative. It is in both Journal's and author's best interest to use terms suitable. For indexing and word search. If there are no such terms in the title, the author is strongly advised to add a subtitle. The title should be given in English as well. The titles precede the abstract and the summary in an appropriate language.

Letterhead Title

The letterhead title is given at a top of each page for easier identification of article copies in an Electronic form in particular. It contains the author's surname and first name initial .article title, journal title and collation (year, volume, and issue, first and last page). The journal and article titles can be given in a shortened form.

Author's Name

Full name(s) of author(s) should be used. It is advisable to give the middle initial. Names are given in their original form.

Contact Details

The postal address or the e-mail address of the author (usually of the first one if there are more Authors) is given in the footnote at the bottom of the first page.

Type of Articles

Classification of articles is a duty of the editorial staff and is of special importance. Referees and the members of the editorial staff, or section editors, can propose a category, but the editor-in-chief has the sole responsibility for their classification. Journal articles are classified as follows:

Scientific articles:

1. Original scientific paper (giving the previously unpublished results of the author's own research based on management methods).

2. Survey paper (giving an original, detailed and critical view of a research problem or an area to which the author has made a contribution visible through his self-citation);

3. Short or preliminary communication (original management paper of full format but of a smaller extent or of a preliminary character);

4. Scientific critique or forum (discussion on a particular scientific topic, based exclusively on management argumentation) and commentaries. Exceptionally, in particular areas, a scientific paper in the Journal can be in a form of a monograph or a critical edition of scientific data (historical, archival, lexicographic, bibliographic, data survey, etc.) which were unknown or hardly accessible for scientific research.

Professional articles:

1. Professional paper (contribution offering experience useful for improvement of professional practice but not necessarily based on scientific methods);
2. Informative contribution (editorial, commentary, etc.);
3. Review (of a book, software, case study, scientific event, etc.)

Language

The article should be in English. The grammar and style of the article should be of good quality. The systematized text should be without abbreviations (except standard ones). All measurements must be in SI units. The sequence of formulae is denoted in Arabic numerals in parentheses on the right-hand side.

Abstract and Summary

An abstract is a concise informative presentation of the article content for fast and accurate Evaluation of its relevance. It is both in the Editorial Office's and the author's best interest for an abstract to contain terms often used for indexing and article search. The abstract describes the purpose of the study and the methods, outlines the findings and state the conclusions. A 100- to 250-Word abstract should be placed between the title and the keywords with the body text to follow. Besides an abstract are advised to have a summary in English, at the end of the article, after the Reference list. The summary should be structured and long up to 1/10 of the article length (it is more extensive than the abstract).

Keywords

Keywords are terms or phrases showing adequately the article content for indexing and search purposes. They should be allocated heaving in mind widely accepted international sources (index, dictionary or thesaurus), such as the Web of Science keyword list for science in general. The higher their usage frequency is the better. Up to 10 keywords immediately follow the abstract and the summary, in respective languages.

Acknowledgements

The name and the number of the project or programmed within which the article was realized is given in a separate note at the bottom of the first page together with the name of the institution which financially supported the project or programmed.

Tables and Illustrations

All the captions should be in the original language as well as in English, together with the texts in illustrations if possible. Tables are typed in the same style as the text and are denoted by numerals at the top. Photographs and drawings, placed appropriately in the text, should be clear, precise and suitable for reproduction. Drawings should be created in Word or Corel.

Citation in the Text

Citation in the text must be uniform. When citing references in the text, use the reference number set in square brackets from the Reference list at the end of the article.

Footnotes

Footnotes are given at the bottom of the page with the text they refer to. They can contain less relevant details, additional explanations or used sources (e.g. scientific material, manuals). They cannot replace the cited literature.
The article should be accompanied with a cover letter with the information about the author(s): surname, middle initial, first name, and citizen personal number, rank, title, e-mail address, and affiliation address, home address including municipality, phone number in the office and at home (or a mobile phone number). The cover letter should state the type of the article and tell which illustrations are original and which are not.

Address of the Editorial Office:

Enriched Publications Pvt. Ltd.
S-9,IInd FLOOR, MLU POCKET,
MANISH ABHINAV PLAZA-II, ABOVE FEDERAL BANK,
PLOT NO-5, SECTOR -5, DWARKA, NEW DELHI, INDIA-110075,
PHONE: - + (91)-(11)-45525005

Note